Cosmic ray showers and particle physics at energies 10^{15}–10^{18} eV*

T. K. Gaisser

Bartol Research Foundation of The Franklin Institute, University of Delaware, Newark, Delaware, 19711

R. J. Protheroe, K. E. Turver, and T. J. L. McComb

Department of Physics, University of Durham, Durham, England

Observations of extensive air showers generated by interactions of cosmic rays high in the atmosphere provide our only source of information about hadronic interactions above 1000 TeV. We review the current status of such experiments, discuss thier implications for particle physics, and also note the astrophysical implications of the results. We place considerable emphasis on a description of the experiments and of the calculations required for their interpretation. We are motivated particularly by the relevance of existing air shower data both to the proposed new generation of accelerators, which will explore the region up to ~1000 TeV, and to a new generation of air shower experiments, which has the potential to observe longitudinal development of individual showers with energies up to 10^{21} eV.

CONTENTS

*Research supported in part by the U. S. National Science Foundation and by the U. K. Science Research Council.

INTRODUCTION

There is considerable contemporary interest in particle interactions at those high energies accessible only through the study of cosmic ray extensive air showers (EAS), i.e., $E \gtrsim 1000$ TeV. The interpretation of air shower data, however, involves consideration also of the nature of the primary particles, which, because of their exceedingly low flux, cannot be directly observed at these high energies. It is our intention here to seek to clarify and, as far as possible, to separate the particle physics and astrophysics aspects of air shower studies. Success in this will ultimately lead to information on the primary particle mass—a long-standing goal of high-energy astrophysics. It can also be expected to lead to information about gross features of particle interactions at energies up to 10^{18} eV, a region which may never be explored by accelerators. We emphasize at the outset, however, that it is not possible on the basis of existing work to disentangle completely the particle physics from the astrophysical implications of extensive air showers. Thus an important goal of this review is to delineate the direction in which further experiment and analysis is required.

A review and clarification of the situation for $10^{15} < E < 10^{18}$ eV is particularly timely from the point of view of high-energy physics for several reasons. (1) The design of the new generation of accelerators presently under consideration may benefit from hints about the behavior of particles at high energies. (2) Results on multiparti-

Copyright ©1978 American Physical Society

cle production at 100–1000 GeV are now clearly in focus, and scaling (Feynman, 1969; Benecke *et al.*, 1969) provides a well-defined extrapolation that is amenable to test at high energy. (3) This is especially so since it has become clear recently that nuclear effects in the light atmospheric nuclei will not seriously obscure matters. In addition, knowledge of the atomic mass number of the primaries of energy 10^{17} to 10^{18} eV is necessary for a full and proper interpretation of the data now available on the primary energy spectrum and arrival directions of these energetic cosmic rays.

A related review of cosmic rays and hadronic interactions from 10 to 1000 TeV has been given by Gaisser and Yodh (1978). In this medium[1]-energy range somewhat more direct information about single interactions is available. In contrast, the flux of primary cosmic rays above 10^6 GeV is so low (~10^2 particles/m^2/sr/year at the top of the atmosphere) that their interactions can only be studied indirectly by making use of the upper atmosphere as the target and sampling the resulting cascade deep in the atmosphere with arrays of large area. Since, in general, many interactions intervene between the initial collision and the observed cascade particles, extensive modelling and computer simulation are required to interpret the results in terms of fundamental aspects of the primary cosmic rays and the elementary particle interactions.

The approach we employ in this paper differs from that in earlier work both by ourselves (Gaisser and Maurer, 1972; Fishbane *et al.*, 1974; Gaisser, 1974a; and Turver, 1975) and other workers (Wdowczyk and Wolfendale, 1972, 1973) in a number of ways. Firstly, we here place emphasis on interpretation of recently reported experiments at the highest energies ($\geq 10^{17}$ eV). These experiments provide data on well-defined and measured features of large air showers. Secondly, it is our aim to tailor detailed simulations specifically for these observed quantities, thus removing ambiguities associated with the extrapolation and interpretation of data. Further, we adopt a similar procedure in our treatment of data from earlier measurements at lower energies (the bases of many previous interpretations). As far as possible, we tailor simulations for direct comparison with the basic data of the original experiments as well as with derived quantities, which may sometimes be conceptually simpler. This approach has been used in reporting the results of some recent experiments (Hammond *et al.*, 1977) and in a preliminary interpretation of these and other experiments (Gaisser, Protheroe, and Turver, 1977). Our goal here is to apply the analysis systematically to a wider range of EAS data in order to present a coherent picture of the current status of cosmic rays and particle physics above 1000 TeV.

To set the theme, we address ourselves to the question, is the development of air showers at energies up to 10^{18} eV consistent with particle physics scaled up in energy from accelerator data at 100–1000 GeV? Careful comparison of detailed simulations with a broad range of observational data suggests that many aspects of shower development are indeed consistent with scaling for particle physics. For at least two aspects of EAS data, however, scaling provides a plausible explanation only if the primaries contain a significant fraction of heavy nuclei. Indeed, we find that scaling and heavy primaries can account, at least qualitatively, for a wide variety of recent measurements of Čerenkov radiation in large showers as well as for the observed rapid development of the electron cascade and the large magnitude of the muon-to-electron ratio.

Certain other aspects of showers, particularly the energy dependence of the μ/e ratio and the lateral distributions of low-energy particles, are inconsistent with Feynman scaling (Feynman, 1969) even if the primaries are all heavy nuclei. Many authors (e.g., Olejniczak *et al.*, 1977; Barrett *et al.*, 1977; Vernov *et al.*, 1977, and Bourdeau *et al.*, 1977) have argued that these difficulties are symptomatic of a fundamental change or threshold in the particle physics somewhere between the highest accelerator energy (~2 TeV) and EAS energies (~1000 TeV). Such a drastic change (involving, for example, breakdown of scaling in the fragmentation region and $\langle n \rangle \propto E^{1/2}$) is by no means ruled out by existing EAS data. Here we take a more conservative point of view and ask whether less drastic modifications in the particle physics (for example, breakdown of scaling only in the pionization region and/or an energy-dependent cross section) together with a primary composition weighted suitably toward heavy nuclei can account for existing EAS data.

In Sec. I we shall review the essential arguments so far presented which have led to the strong suggestion that shower development based on a scaling model for particle production is unacceptable if the primaries are all protons. Next, we shall describe in Sec. II in some detail the model for particle production and scaling and the scope of the cascade propagation procedures which we have employed to interpret EAS data. We shall then describe in Sec. III the results of applying a model of scaling with a variety of assumed primary spectra to a well-defined but broadly based body of data from experiments at energies around 10^{17}–10^{18} eV. In Sec. IV we shall consider the effects of scaling with various primary compositions on gross features of showers in the range 10^{15}–10^{17} eV, with particular emphasis on possible problems associated with earlier interpretations of these data.

The approach in Secs. III and IV is to compare calculations based on the Feynman scaling hypothesis with EAS data, for a variety of mean primary masses. In Sec. V we attempt to evaluate the implications of residual discrepancies between calculated and observed showers for models of strong interactions, and it is noted that use of the Landau (1953) model leads to significant improvement while maintaining scaling in the fragmentation region. In Sec. VI we briefly summarize implications for primary composition that follow if scaling in the fragmentation region (Benecke *et al.*, 1969) is enforced at EAS energies. We contrast results with primaries of $A = 1$, $A = 10$, and $A = 56$, which are typical respectively of interstellar matter, ordinary (i.e., low-energy) cos-

[1]The use of the terminology "low, medium, and high energy" to refer, respectively, to <1 TeV, 1–1000 TeV, and >1000 TeV has been introduced by Weinberg (1977) in the context of unified theories of particle interactions.

mic rays, and highly evolved material[2]. The possible effects of fluctuations in the presence of a mixed composition are mentioned, though we do not attempt to deal with them quantitatively in this paper. In the conclusion we point out the consequences for a determination of the primary spectrum up to 10^{15} eV of a new generation of accelerators which will explore particle interactions up to this energy. New directions in air shower experiment and calculation are also discussed.

I. GENERAL FEATURES OF AIR SHOWERS

An extensive air shower is the atmospheric cascade produced by a single cosmic ray primary with energy large enough to produce a coherent, detectable flux of particles at an observation level deep in the atmosphere. The primary nucleus collides with a target air nucleus high in the atmosphere, producing secondary mesons and a fragment nucleon (or nucleons if the incident particle is a heavy nucleus). Neutral pions decay immediately to two photons which initiate electromagnetic cascades in the atmosphere. Nucleons and some charged pions interact again to sustain the hadronic core of the cascade. Other charged pions decay to muons, contributing to the development of the muonic component of the cascade. The hadronic core continues to feed the electromagnetic and muonic components as it penetrates into the atmosphere.

The cascade equations that govern the shower development and their connection with particle physics will be discussed in detail in the following section. Briefly, however, given a specific model for the inclusive cross section for production of mesons and nucleons in hadron–air nucleus collisions, one calculates the fluxes of electrons, muons, and hadrons that can be measured. Comparison between aspects of calculated and observed showers then allows one to draw conclusions about the initial assumptions.

Feynman scaling (Feynman, 1969) or the hypothesis of limiting fragmentation (Benecke *et al.*, 1969) provides a simple algorithm for extrapolating data on hadronic interactions from 100–1000 GeV (where it is well determined at accelerators) to cosmic ray energies in such a way that very general theoretical expectations about strong interactions can be tested over a range of more than three decades in center-of-mass energy.

A. Electromagnetic component

The most populous particles in cosmic ray air showers are the electrons, and the growth of the electron cascade is a fundamental characteristic of the air shower. This cascade development depends primarily upon the momentum distribution of the secondary π^0's in energetic p-air and π-air interactions. The cascade shows a growth, maximization, and decay as the energy of the shower is degraded. The single most useful indicator of

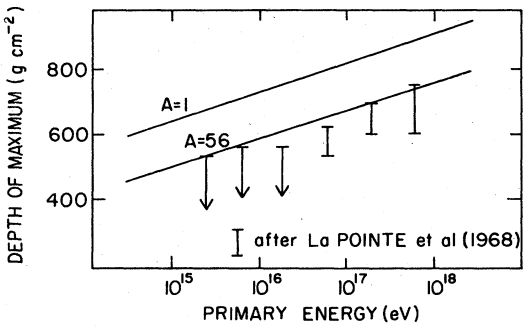

FIG. 1. The variation of the average depth of electron cascade maximum with primary energy.

cascade development is the depth of maximum development of the cascade in the atmosphere.[3]

Interpretations to date (e.g., Wdowczyk and Wolfendale, 1972; Gaisser and Maurer, 1972), suggest that the cascades develop with their maxima significantly higher in the atmosphere than can readily be accounted for if the primary particles are protons and the momentum distribution of secondaries follows scaling. This conclusion is illustrated by Fig. 1, which shows data for depth of maximum compared to the scaling calculations for $A = 1$ and $A = 56$ as the primary mass number.

B. Muonic component

An indication of the energy degradation and the sharing of energy between charged and neutral pions in a cascade is the muon content of a shower. In contrast to the electron cascade, the muon cascade grows and maximizes, but decays only slowly, as a result of the stability of the muon and its small cross section for radiation and pair production. The ratio of mu-

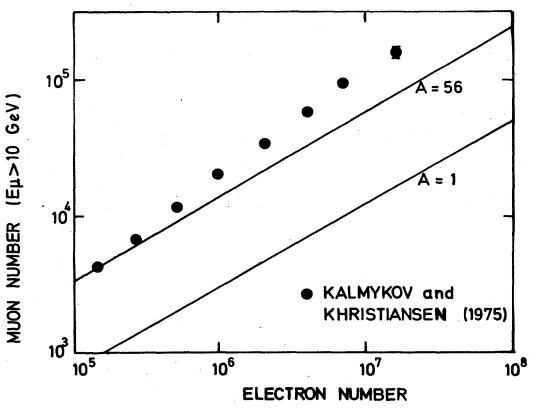

FIG. 2. The variation of number of muons of energy >10 GeV as a function of average electron shower size.

[2]Iron is chosen as the nominal heavy nucleus for calculation simply because it has the highest binding energy per nucleon. Other heavy primaries would lead to similar showers characterized by small fluctuations and early development.

[3]Although depth of maximum is difficult to observe directly with most existing experiments, it can be shown to be well-correlated with several other shower observables (Dixon, and Turver, 1974) and is readily calculable.

on number to electron number is thus an indication of overall shower development. The data of Khristiansen *et al.* (1971) on $N_\mu - N_e$ dependences have frequently been interpreted as strong evidence against the validity of the scaling concept if a beam of primary protons is assumed, as illustrated by Fig. 2.

Here our calculations refer to showers of fixed primary energy, whereas the measurements are for showers of fixed size. As a consequence of this, our values represent upper limits. As explained later, the correct calculation for protons will be even farther from the data, while the curve for iron will be essentially unaffected.

C. Tentative interpretation

We note that these discrepancies may be alleviated by many changes in assumed primary particle mass and/or interaction models which result in a decrease in the depth of maximum of electron cascade of ~100 g cm^{-2}. As is illustrated in Figs. 1 and 2, one such possibility is the assumption of a beam of heavy nuclei as primaries. Thus a fundamental problem with the interpretation of EAS is to disentangle astrophysical aspects (e.g., composition of cosmic rays) from the particle physics.

It should also be emphasized, however, that neither the average depth of maximum of showers of fixed primary energy, nor the muon content (N_μ/N_e) is a directly measured quantity. Both are inferred from measurements of densities of particles in showers with significant fluctuations from shower to shower in primary energy, in depth of first (and subsequent) interaction, in location of the core relative to the detectors, etc. In these circumstances, the possibility of systematic effects cannot always be ruled out. Such possibilities motivate our efforts to produce detailed simulation results which are directly comparable to the measured quantities.

II. CASCADE THEORY AND SHOWER MODELLING

The simulation of air showers incorporates hadronic cross sections into the calculation of the hadronic cascade as described, for example, by Gaisser (1974b), using scaling or some alternative to extrapolate from accelerator to EAS energies. The articulation of the showers follows broadly the pattern established in earlier work of Dixon, Earnshaw, *et al.* (1974) and comprises five sections. Firstly, we consider the generation by the hadron cascade of the energy spectrum of pions produced at various depths in the atmosphere. Next, the high-energy (>75 GeV) electron–photon cascade is followed in one dimension using cascade theory under approximation *A* (Rossi and Greisen, 1941). This in turn is followed by calculations in 4-*D* of the e-γ component and the Čerenkov light based upon detailed Monte Carlo electron–photon cascades (using the scheme first suggested by Butcher and Messel, 1960). The propagation of the muon component is considered in detail using Monte Carlo methods.

A. The hadronic cascade

The cascade equations governing the development of the hadronic core of an EAS of primary energy E_0 are

$$\frac{dN_{E_0}(E,y)}{dy} = -\frac{N_{E_0}(E,y)}{\lambda_N(E)} + \int_E^\infty \frac{F_{NN}(E,E')}{E}\frac{N_{E_0}(E',y)}{\lambda_N(E')}\,dE' \tag{2.1}$$

and

$$\frac{d\Pi_{E_0}(E,y)}{dy} = -\Pi_{E_0}(E,y)\left[\frac{1}{\lambda_\pi(E)} + \frac{\epsilon_\pi}{Ey\cos\theta}\right] + \int_E^\infty \frac{F_{N\pi c}(E,E')}{E}\frac{N_{E_0}(E',y)}{\lambda_N(E')}\,dE' + \int_E^\infty \frac{F_{\pi c,\pi c}(E,E')}{E}\frac{\Pi_{E_0}(E',y)}{\lambda_\pi(E')}\,dE', \tag{2.2}$$

where $N_{E_0}(E,y)dE$ and $\Pi_{E_0}(E,y)dE$ are, respectively, the average numbers of nucleons and of charged pions at atmospheric depth y, (measured along the shower axis in g/cm^2) and of energy between E and $E+dE$ due to a primary nucleon of energy E_0. Here $\lambda_\pi(E)$ and $\lambda_N(E)$ are, respectively, the pion and the nucleon interaction length in air. In general these are taken to be energy dependent to reflect the possible energy dependence of the p–air and π–air cross section. The quantity $(\epsilon_\pi dy)/(Ey\cos\theta)$ is the probability that a pion along the shower axis with zenith angle θ decays in dy. Here $\epsilon_\pi \equiv h_0 m_\pi/\tau_0 \cong 128$ GeV, where τ_0 is the pion lifetime, m_π its mass, and $h_0 \sim 7$ km is the scale height of the atmosphere. It is clear that the cascade equations as written include only nucleons and charged pions (π^0's always decay before interacting and thus contribute only to the electromagnetic cascade).

Separate treatment of other species would require further coupled equations; therefore we have for simplicity treated kaons as pions and strange baryons as nucleons. Moreover, $N\bar{N}$ production has been neglected. In particular cases, keeping track separately of K and $N\bar{N}$ production can be important, as for example in calculating μ^+/μ^- or in calculating the ratio of neutral to charged energetic hadrons in showers. We assume, however, that if K/π and $N\bar{N}/\pi$ ratios do not increase more rapidly than expected on the basis of accelerator data that these simplifications are unimportant for the longitudinal development of EAS. (See, e.g., Gaisser and Rudolf, 1976, for a discussion of $N\bar{N}$ production in EAS. We expect that separate treatment of K decay will lead to a 10%–20% increase in the flux of muons.) Grieder (1977a and b) has shown, however, that if $N\bar{N}$ production increases much more rapidly, then it can significantly affect such gross measures of shower development as depth of maximum. This point should be borne in mind if the Centauro events (Lattes *et al.*, 1975—see Gaisser and Yodh, 1978, for a review) are substantiated. These events suggest a possible dominance of nucleonic (or nonpionic) secondaries around 1000 TeV.

High-energy physics enters the cascade equations only through the inelastic hadron-air cross sections

$$\sigma^{\text{inel}}_{p\text{-air}} \cong \frac{2.41\times10^4(\text{mb gm/cm}^2)}{\lambda_{p\text{-air}}(\text{gm/cm}^2)} \tag{2.3a}$$

and

$$\sigma^{\text{inel}}_{\pi\text{-air}} = \frac{2.41\times10^4(\text{mb gm/cm}^2)}{\lambda_{\pi\text{-air}}(\text{gm/cm}^2)}\,, \tag{2.3b}$$

and through the production cross sections, F_{NN}, $F_{N\pi}$ and $F_{\pi\pi}$, etc. Here

$$F_{ab}=\frac{\pi}{\sigma^{\text{inel}}}\int E\frac{d\sigma_{ab}}{d^3p}\,dp_T^2\cong E_b\frac{dN_b}{dE_b}\ , \tag{2.4}$$

and $E(d\sigma_{ab}/d^3p)$ is the Lorentz invariant inclusive cross section for the process $a+$air nucleus $\rightarrow b+$anything. Given a theory which predicts $F_{ab}(E,E_0)$ and $\sigma_{a\text{-air}}$, shower observables can be calculated from known decay properties of mesons, electromagnetic cascade theory, properties of the atmosphere, etc.

The computer program for the hadron cascade is divided into two sections which employ Monte Carlo and analytic techniques. Nucleons of all energies and pions above a prescribed threshold (chosen here as $10^{-3}\times$ primary energy) are "followed" in the Monte Carlo section. In N-air nucleus collisions the energy of the leading nucleon is first sampled from F_{NN} and then pions are sampled from $F_{N\pi^c}$ (produced). The cascade resulting from particles produced with energies below the threshold is treated by numerical integration of the diffusion equations that govern the development of the shower.

B. Nucleus-nucleus collisions

As suggested in the introduction, an important possibility is that many showers may be generated by primary nuclei with $Z>1$. We therefore describe how nuclear fragmentation and pion production in collisions between nuclei with $Z>1$ may be calculated.

In many calculations of nucleus-initiated EAS the superposition model has been used (de Beer *et al.*, 1966; Hillas, 1965; Gaisser, 1974a; etc.). This model assumes that the shower from a primary nucleus of energy E and mass A is equivalent to the sum of A nucleon-initiated showers of primary energy E/A. This simple treatment has been shown in earlier work (Dixon and Turver, 1974) to underestimate fluctuations in cascade development. The present treatment of primary nuclei is based on that of Dixon, Turver, and Waddington (1974), which uses data for the fragmentation similar to that described in detail by Freier and Waddington (1975).

The problem is to calculate the depths at which each of the A nucleons first interacts, after which the simulation proceeds as described for nucleon-initiated showers. The depth at which the primary interacts is sampled from a distribution with mean free path given by Cleghorn *et al.* (1968). In the interaction the primary nucleus breaks up into fragment nuclei, α particles and nucleons. A fraction of the nucleons released in the fragmentation interact with the target air nucleus to produce pions. Dixon *et al.* assumed this fraction to be 0.25 but measurements by Tomaszewski and Wdowczyk (1975) suggest the fraction of interacting nucleons should be ~0.75 for medium nuclei decreasing to 0.5 for heavy nuclei. The higher values have been used in the present work.

This treatment of fragmentation is of particular importance in studies of fluctuations in showers. For calculations of average characteristics, which is our primary concern in this review, the superposition model would suffice (Tomaszewski and Wdowczyk, 1975).

C. Scaling model for inclusive cross sections

In the main part of this review we shall adopt Feynman scaling (Feynman, 1969) as the standard model for the inclusive cross sections. With this very powerful assumption

$$F_{ab}(E,E_0)\rightarrow F_{ab}(E/E_0)\,. \tag{2.5}$$

Thus F_{ab} can be determined from experiments at the highest available accelerator energies and scaled up to EAS energies for the cascade calculation. Comparison between calculated and observed showers then tests the Feynman scaling over a range of some six decades in lab energy.

Data for F_{ab} are normally given in the c.m. system as a function of the variable x defined by $x\equiv 2P_{\parallel}^{\text{c.m.}}/\sqrt{s}$, where $\sqrt{s}$ is the total c.m. energy. The transformation to the lab is straightforward. For secondaries with $E^2\gg\mu_\perp^2$ and for $E_0\gg 1$ GeV, a good approximation to the Feynman variable is given by

$$x\cong E/E_0-\frac{\mu_T^2}{2m_pE}\ , \tag{2.6}$$

where $\mu_T=\sqrt{m^2+p_T^2}$ is an rms transverse mass of the secondary ($\mu_T\cong 0.42$ GeV/c for a pion). If Feynman scaling holds at $x=0$ so that $F(0)=$ constant, then for $E\gg\mu_T^2/2m_p$, Feynman scaling implies scaling in the lab variables, as in Eq. (2.5).

The distributions used for $F_{N\pi^c}$ and for $F_{\pi^c\pi^c}(\pi^c$ = charged pion) are shown in Figs. 3 and 4. These distributions are based on accelerator data as described by Fishbane *et al.* (1974) and Gaisser (1974b). $F_{\pi^c\pi^c}$ is divided into two components since it is necessary to account separately for a single "leading" pion and produced pions within the Monte Carlo calculation of the hadronic cascade. (The separation has been discussed by

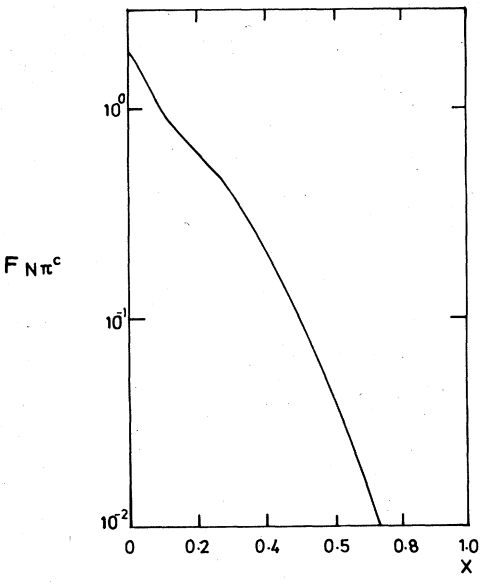

FIG. 3. The inclusive distribution for the production of charged pions in nucleon–nucleon collisions employed in the present work.

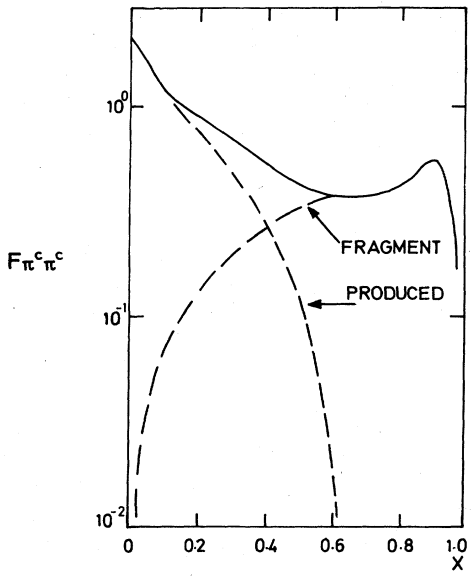

FIG. 4. The inclusive distribution for the production of charged pions in pion–nucleon collisions used in the present work showing the distributions for the leading pion and the produced pions.

Gaisser, 1974b, and is based on an analogy to the leading nucleon in $N+N\to N+X$.) For the "standard scaling model", we have assumed $F_{N\pi^0}=\frac{1}{2}F_{N\pi^c}$ and $F_{\pi^c\pi^0}=\frac{1}{2}F_{\pi^c\pi^c}$. There is adequate experimental justification for the first assumption but the data (Whitmore, 1976) on $\pi^\pm P\to\pi^0 X$ are ambiguous. They are also consistent with the "leading" pion being neutral or charged with equal probability, leading to $F_{\pi^c\pi^0}\neq\frac{1}{2}F_{\pi^c\pi^c}$. The consequences of this possibility for EAS development have been tested and found to be unimportant.

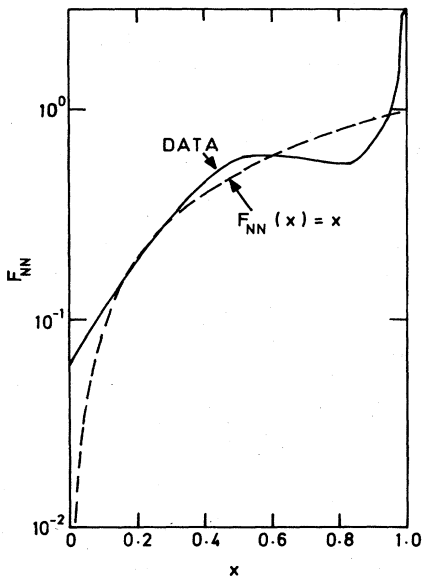

FIG. 5. The inclusive distribution of fragment nucleons in nucleon–nucleon collisions compared with that used in the present work (dashed line).

The distribution $F_{NN}(x)$ is shown in Fig. 5. In the simulations we have actually used the simplified form, $F_{NN}(x)=x$. The effect of this simplification has been checked and found to be negligible. It is appropriate here to mention two points about the relation of the invariant cross sections to quantities normally used by cosmic ray physicists to characterize nuclear interactions.

(1) The nucleon distribution $F_{NN}(x)$ is closely related to the lab inelasticity distribution. It can be shown that the inelasticity distribution is given by

$$\frac{dn}{dK}=\frac{F_{NN}(1-K)}{1-K}\ ,$$

where

$$K\equiv\frac{E_0-E_N}{E_0}\ ,$$

and the distribution is normalized to unity. Here E_0 and E_N are the lab energies of the incident and the scattered nucleon in a nucleon-air nucleus collision.

(2) The growth with energy of the average multiplicity is closely related to $F(x=0)$ in most models. From Eq. (2.4) one has, for example, for the pion multiplicity in nucleon initiated reactions,

$$\langle n_\pi\rangle\cong\int\frac{F_{N\pi}(x)}{\sqrt{x^2+(4\mu_1^2/s)}}\,dx\ ,$$

where $\mu_1^2=\langle p_T^2\rangle+m_\pi^2$. If $F(x)$ is sufficiently well-behaved near $x=0$, then

$$\langle n\rangle\cong F(0)\ln s+\text{const.}$$

The proton–proton cross section has been observed (Amaldi *et al.*, 1973, Amendolia *et al.*, 1973) to increase from 100 to 2000 GeV and beyond (Yodh, Pal and Trefil, 1972; Amaldi *et al.*, 1977), with a corresponding increase in $\sigma_{p\text{-air}}$, and one of the principal questions in particle physics is whether and how this increase continues. Various extrapolations of the accelerator data on cross sections are available; preferred values for the interaction length inferred at 10^{17} eV differ by less than 50% from the values customarily employed in cosmic ray calculations. We have adopted values of 80 gcm^{-2} and 120 gcm^{-2} for $\lambda_{p\text{-air}}$ and $\lambda_{\pi\text{-air}}$, respectively, for the standard model, and we postpone to Sec. V a discussion of the effects of various assumptions about the energy dependence of $\sigma_{p\text{-air}}$ and $\sigma_{\pi\text{-air}}$.

Motivated by results of several recent experiments (e.g., Halliwell *et al.*, 1977) which show that intranuclear cascading is minimal or absent for fast secondaries produced in collisions on nuclear targets, we ignore nuclear target effects for the light atmospheric nuclei relevant to EAS. The consequences of including modifications due to the nuclear target are model dependent in that there are several rather different models that can account for the observed absence of cascading (e.g., Berlad *et al.*, 1976; Capella and Krwczyki, 1977; see Andersson, 1976, for a review). We have not attempted to assess the possible consequences of these models for EAS development. We note that the low-energy muon component may show some sensitivity to this effect.

D. Electromagnetic cascade

The electron cascade has in the past customarily been derived from solutions of the cascade equations under Approximation B. Such solutions are simple but make difficult the precise representation of the threshold effects for the production of Čerenkov radiation and the accurate allowance for the lateral spread of the electrons. Where energy thresholds are important, we use the "Approximation A + Monte Carlo" approach to be described below.

Energetic electrons and photons (>75 GeV) have been considered using cascade theory under Approximation A (Rossi and Greisen, 1941). The development of the e-γ cascade at energies <75 GeV has been followed in space and time using Monte Carlo methods for cascading developed originally by Butcher and Messel (1960) and Baxter (1969) and modified by Smith and Browning (1974, unpublished) and Allan *et al.* (1975). The lateral development of the shower is based upon propagation under the influence of Coulomb scattering and the distortion by the geomagnetic field (here chosen to be appropriate to the Haverah Park array coordinates 54°N, 2°W).

E. Čerenkov radiation from the electron cascade

This simulation follows the electron–photon cascade in detail in a realistic atmosphere, as described above. The production of Čerenkov radiation ($280 < \lambda < 600$ nm) and the subsequent (wavelength-dependent) absorption in the atmosphere as a result of ozone absorption, aerosol attenuation, and Rayleigh scattering according to the data of Elterman (1968) are considered.

In calculating the precise form of the temporal characteristics of the light pulse it is necessary to assume a response function for the light detector. We have chosen to consider here a system which responds to a narrow pulse of light with a pulse shape characterized by a rise time of 9 ns and a FWHM (full width at half maximum) of 19 ns. This we consider from experimental experience—see Hammond *et al.* (1977)—to be typical of a system having a bandwidth appropriate to an array of well-separated detectors necessary for measurements in large cosmic ray showers.

Comparison of the characteristic angular spread of the electron cascade—of prime importance to Čerenkov light studies—from this and other simulations has been made by Hammond *et al.* (1977), who find good agreement among the various calculations.

F. Muon propagation

The propagation in 4-D of those muons arising from the decay of charged pions is considered using Monte Carlo methods. Allowance is made for the following processes:

(1) The transverse momentum imparted to the parent pion. This is chosen from a distribution of the form:

$$f(p_t)dp_t = 25.0 p_t \exp(-5.0 p_t) dp_t .$$

(2) The $\pi - \mu$ decay.
(3) Coulomb scattering of the parent pion and muon.
(4) The interaction between the particle and the geomagnetic field.
and
(5) The distorting effects (particularly important from the point of view of spatial angle studies) of the absorber in typical detectors.

We also allow for the effects of photoproduction of pions as discussed by McComb, Protheroe, and Turver (1977). The pions produced in this process give rise to additional low-energy muons. The effect increases with primary energy and may become important at energies $\gtrsim 10^{18}$ eV.

III. INTERPRETATION OF 10^{17} - 10^{18} eV DATA

Our first application of the simulation described in Sec. II is to the large showers with $E_0 \sim 10^{17}$–10^{18} eV. An important characteristic of these data, most of which have been obtained at the Haverah Park air shower experiment, is the clearly stated and consistent estimate of the primary energy which is available for each shower from the well-established array.

A. Detecting and recording large showers

The requirement when recording showers for astrophysical studies (e.g., measurements of the primary energy spectra and arrival directions) or energetic interaction studies (e.g., measurements of cascade longitudinal development) is to obtain a sample of the times of arrival and particle densities across the shower front in individual showers. At Haverah Park this is done using an array of a relatively small number (7) of large-area (34 m^2) deep-water Čerenkov detectors[4] (Tennant, 1967); we note that this is in contrast to the procedure, e.g., at the Volcano Ranch array (Linsley, 1973), where a large number (79) of small-area (1 m^2) scintillation detectors is employed. In the measurements at Haverah Park the arrival direction of the shower is assumed to be the normal to a plane fitted to the arrival times of the signals at widely spaced (~800 m) detectors. The center of symmetry of the shower (i.e., the core) is found by assuming that the variation of detector response with distance from the core (i.e., the lateral distribution) is monotonic. The procedure for core location uses computer optimization techniques.

The measure of primary energy adopted at Haverah Park for showers of ~10^{17} eV is the ground parameter $\rho(500)$, the response of a deep-water Čerenkov detector to shower particles at 500 m from the air shower core. This has been described in detail by Edge *et al.* (1973). Since these detectors are sensitive to both the electron-photon component and the muon component they are calibrated by their response to single muons, and $\rho(500)$ is therefore measured in units of vertical equivalent muons per square meter. The essential reason (first suggested by Hillas *et al.*, 1971a) that $\rho(500)$ is well correlated with primary energy on a shower-by-shower basis (despite fluctuations in the development of individuals) is that at ~500m from the core the detector response arises from

[4]The deep-water detectors are sensitive to Čerenkov radiation produced in the water of the detector by muons and electrons. They are not sensitive to atmospheric Čerenkov light.

approximately equal contributions from the electron-photon and muon components. Furthermore, changes in longitudinal cascade development lead (regardless of shower models) to anticorrelated changes in the muon and electromagnetic components. In addition, $\rho(500)$ is particularly well measured by this array.

Some data reported here, e.g., the shape of the deep-water Čerenkov detector structure function, were obtained with the large area detectors which form the prime shower detection facility. Other data have been recorded by additional types of detector exposed in the "beam" of well-measured showers available from the prime facility. These additional detectors have included a large-area magnet spectrograph for the measurement of the momentum distributions of muons, various muon number density detectors (currently a total sensitive area of 50 m^2 is available), and, in recent years, an array of eight air Čerenkov detectors.

We calculate the Čerenkov light produced by electron-photon cascades and by muons within the deep-water detectors for each computed shower in order to assign values of $\rho(500)$ appropriate to Haverah Park to simulated showers. The simulations have been tailored to reproduce the conditions appropriate to each observation considered, thus reducing the uncertainties which arise when simulations of a more general nature are compared with specific measurements. We therefore attach extra weight to the comparison of these simulations with a range of measurements of the electron, muon, and atmospheric Čerenkov light components made at Haverah Park in showers with the given primary energy estimate $\rho(500)$.

B. The muon component

1. Lateral distribution

Measurements have been made at Haverah Park of the lateral distribution of muons of energy in excess of 300 MeV and 1000 MeV by Strutt (1976) and Dixon, Machin, *et al.* (1974) respectively. The measurements were made in showers incident from within 30° of the zenith, and of known $\rho(500)$. The data are reduced to refer to showers from the zenith. In the experiments, consideration was given to the effects of detector saturation (occurring when the detector is close to the core); in the simulations the effects of core mislocation have been considered. Both of these features are known to cause distortion of the structure function. The data from these experiments are shown in Fig. 6, where they are compared with the results of our simulations. A satisfactory representation is given both of the structure function shape and absolute muon densities at core distances $\gtrsim$100 m, by the scaling model. Other models of particle physics give similar representations of these data. No marked sensitivity to primary mass is observed. At core distances <100 m, the fit of the simulated structure function to the observations is less satisfactory. This may be a consequence of inadequate allowance for core mislocation effects (which have their maximum effect flattening the structure function near the core) or, in the case of the 1 GeV threshold data, of inaccurate normalization of measurements. (We note that data at distances less than and greater than 100 m were obtained in separate experiments.)

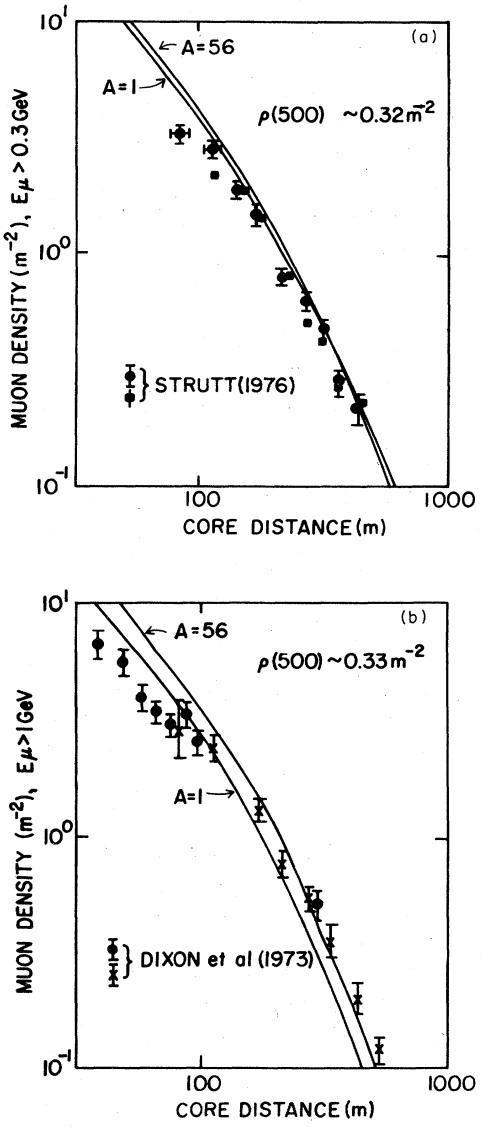

FIG. 6. The lateral distribution functions for low-energy muons of energy in excess of (a) 0.3 GeV and (b) 1 GeV in showers of Haverah Park ground parameter values 0.32 m^{-2} and 0.33 m^{-2}.

2. Momentum spectrum

The differential momentum spectrum of muons at 300 m and 500 m from the shower core have been measured using a magnet spectrograph by Dixon, Machin, *et al.* (1974). The spectra measured in showers incident at less than 30° from the zenith are shown in Fig. 7 and are compared with the results of our simulations using the scaling model with proton and iron nucleus primaries for vertical showers. In particular, we attach significance to the shape of the spectrum; the absolute densities are based directly on the measurements already

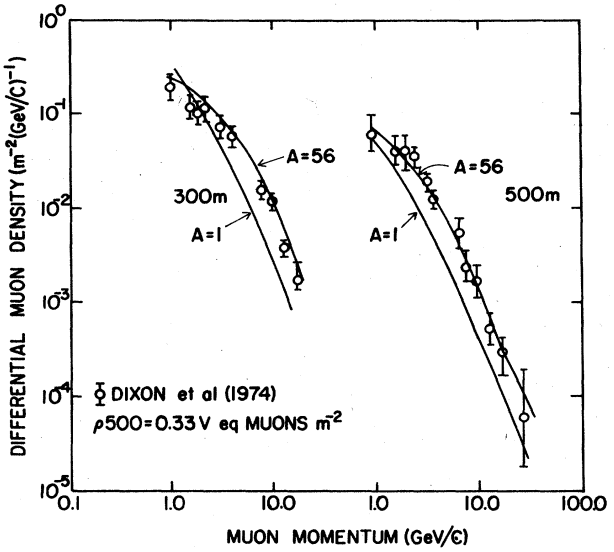

FIG. 7. The momentum spectrum of muons at 300 and 500 m from the core of showers of Haverah Park ground parameter 0.33 m^{-2}.

discussed above. The shape of the spectra predicted for proton primaries is too steep, especially at smaller core distances.

3. Height of origin

The heights or origin of muons (reduced to a common detection energy threshold of 300 MeV) in large showers have been summarized by Earnshaw *et al.* (1973). These heights, which were derived from the spatial and temporal distribution of muons and the geomagnetic distortion of the muon charge ratio in a number of experiments, are shown in Fig. 8. The simulation results using scaling with iron nucleus primaries are found to be in good agreement with the data.

C. Atmospheric Čerenkov radiation

A large proportion of the electrons in showers are sufficiently energetic to emit visible Čerenkov radiation in air. The first measurement of this light was made by Galbraith and Jelley (1953) and subsequent work by Chudakov *et al.* (1960) was confined to showers smaller than ~10^{17} eV.

More recently there have been measurements of photon fluxes present at large core distances in high-energy showers. Such visible photons, primarily from atmospheric Čerenkov radiation, are the most numerous component at core distances of about 200 m in large showers and reach densities of 10^7 photons/m^2 at sea level for showers of energy in excess of 2×10^{17} eV, although climatic conditions may present significant experimental problems in their measurement. The information carried by such photons differs from that contained in the more energetic locally produced photons since the optical signal is derived from all electrons in the shower and so reflects the total development of the shower through the atmosphere; it thus relates well with the primary particle energy and mirrors the longitudinal development of the shower.

1. Lateral distribution

The lateral distribution of the total Čerenkov light signal in near vertical showers of known sea level shower size or of primary energy estimate $\rho(500)$ has been measured by Diminstein *et al.* (1972) and Hammond *et al.* (1977), respectively. The measurement and calculation of the absolute photon flux is demanding, and we here attach greater significance to the shape of the function than to absolute fluxes. A comparison is made in Fig. 9 with the data of Hammond *et al.* (1977) for a given value of $\rho(500)$. The predictions are normalized to the lower energy shower data at 200 m from the core. The solid lines refer to photon densities for a factor of 10 increase in the Haverah Park energy estimator, $\rho(500)$.

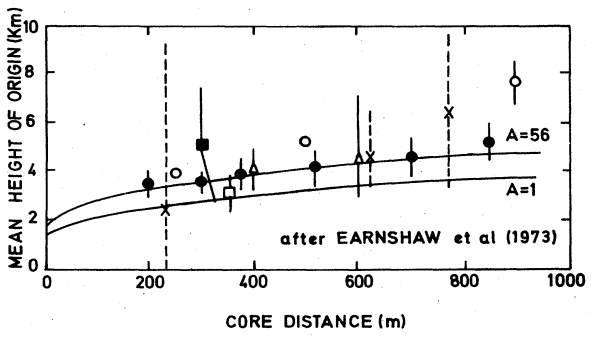

FIG. 8. The mean height of origin of muons of energy >0.3 GeV in showers of primary energy 10^{17} eV.

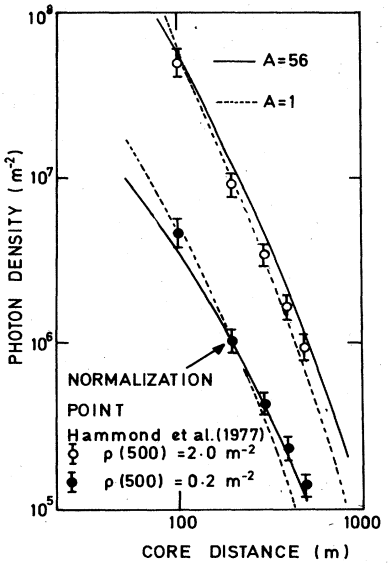

FIG. 9. The average lateral distribution function for air Čerenkov radiation in showers having values of the Haverah Park ground parameter 0.2 and 2.0 m^{-2}.

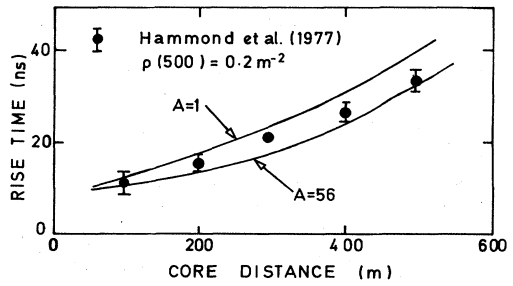

FIG. 10. The average rise time of the air Čerenkov pulses recorded at various core distances in showers having Haverah Park ground parameter value of 0.2 m^{-2}.

2. Pulse shape

The potential of the light pulse shape as an indicator of cascade development was suggested by Boley (1964). Measurements were initiated by Efimov *et al.* (1973) and have been fully exploited by Hammond *et al.* (1977). The average pulse shape, which can be represented by the rise and fall times and the FWHM at known core distances, are shown in Figs. 10, 11 and 12a. Here care has been taken to allow in the calculation for the response of the detectors of the type used by Hammond *et al.* Again, the predictions of the scaling model fit the data for the rising and falling edges of the pulse adequately, independently of the primary mass. For FWHM, however, the data of Hammond *et al.* show a preference for heavy primary nuclei. The preference for heavy primaries is even more noticeable in Fig. 12b, where we show top time, which is defined as the time between 90% of maximum on the rising and falling edges. We note that simulations of Hammond *et al.* show that the top time is correlated with depth of shower maximum, independently of primary mass. Thus the data of Fig. 12 do not necessarily require heavy primaries, but only early development.

The data on FWHM of the pulse reported recently by Kalmykov *et al.* (1976) are also shown in Fig. 12a. When it is noted that these authors have corrected their data for the effects of the bandwidth of their detectors, their data are also seen to be well represented by the present simulations for a detector with zero response time. Here we have indicated by broken lines the predictions

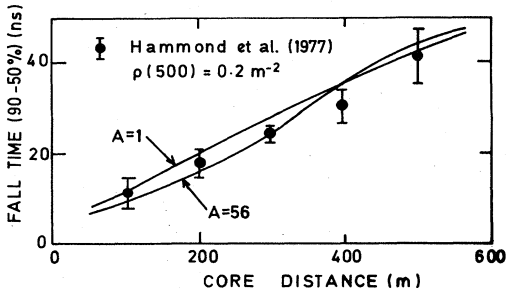

FIG. 11. The average fall times of the air Čerenkov pulses recorded at various core distances in showers having Haverah Park ground parameter 0.2 m^{-2}.

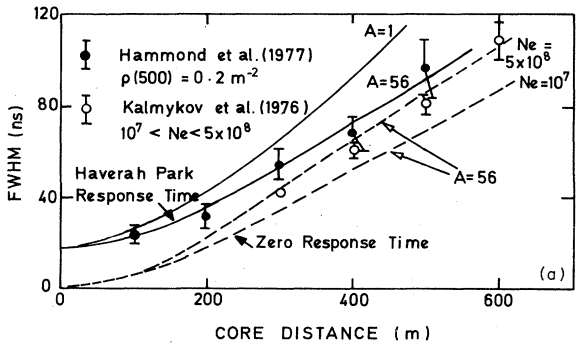

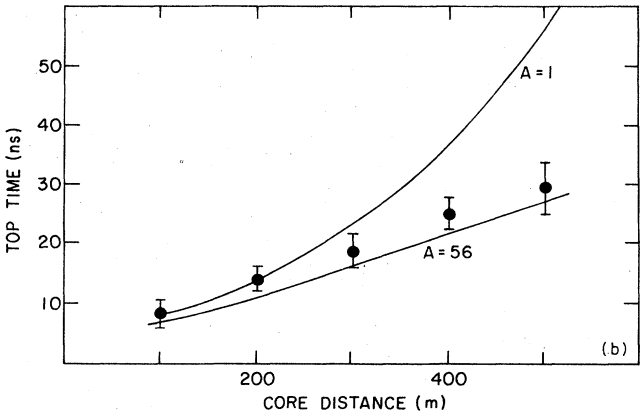

FIG. 12. (a) The average full width at half maximum of the air Čerenkov pulses recorded at various core distances in showers having Haverah Park ground parameter value 0.2 m^{-2}. (b) The same for top time.

for showers with electron number ranging from 10^7 to 5×10^8 particles, to be consistent with the measurements. This is in agreement with the authors' own interpretation (Kalmykov *et al.*, 1977). It is our view that the measurements of the shape of the Čerenkov light pulse, requiring no accurate knowledge of the detector absolute gain (and thus no normalization), provide one of the best tests of models.

3. Curvature of the light front

The depth of initiation of the electron cascade is reflected by the radius of curvature of the atmospheric Čerenkov light front. This can be well measured without the sampling problems which characterize many measurements of the particle front. When the light front is defined as the time at which 10% of the full height of the light signal is achieved, a radius of curvature for measurements in the range 100–500 m from the core of 8.2 km was observed by Hammond *et al.* (1977) in a sample of showers of mean $\rho(500) = 0.90$ vertical equivalent muons m^{-2}. The simulations give a corresponding mean radius of curvature of 6.8 km for proton primaries, and 7.9 km for iron nucleus primaries. As is the case for FWHM and top time, radius of curvature is correlated with depth of shower maximum. Thus any change that decreases depth of maximum increases the radius of curvature.

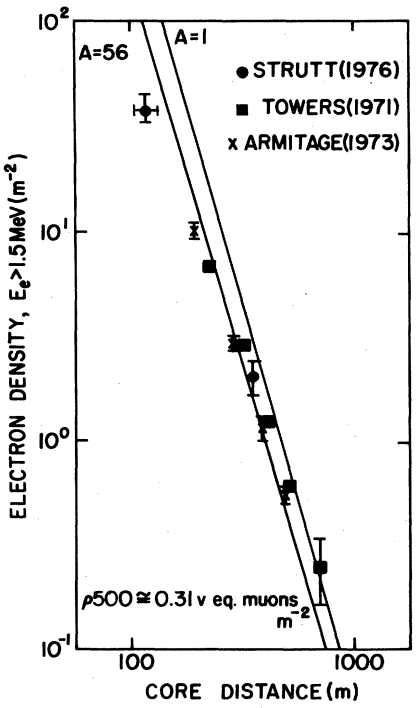

FIG. 13. The average lateral distribution of electrons (energy >4 MeV) in showers having the Haverah Park ground parameter value 0.31 m^{-2}.

D. Lateral distribution of electrons

Measurements of the lateral distribution of electrons have been made by Towers (1971), Armitage (1973), and Strutt (1976) at sea level at Haverah Park for showers of fixed $\rho(500)$ using flashtubes and scintillators. Their data are shown in Fig. 13, where they are compared to the result of our simulation. The calculated lateral distribution structure function is seen to be somewhat steeper than the data. This failure is a persisting problem in the interpretation of shower data, and is not confined to this particular set of measurements and calculations (see, e.g., Hillas *et al.*, 1971b).

The review of data by Atrashkevich *et al.* (1977) and recent measurements by Linsley (1977) provide detailed information on the lateral distribution of all charged particles for showers of fixed N_e. Unfortunately, calculations of lateral distributions in showers of fixed N_e [rather than fixed $\rho(500)$] are not available from our work.

E. Deep-water Čerenkov detector response

The large-area deep-water Čerenkov particle detectors are unique to the Haverah Park array and have been extensively studied over the years (see, e.g., Edge *et al.*, 1973). The lateral distribution of the signal recorded by these detectors (a complicated combination of the electron–photon and muon fluxes) is now well known. The structure function of a shower of $\rho(500) = 1.0$ m^{-2} is shown in Fig. 14, where it is compared to the result of our simulations for a proton and an iron nucleus primary, each with an energy giving the same $\rho(500)$. A further measure of the shape which has been employed at the Haverah Park experiment, particularly for the investigation of fluctuations, is $B(100)$, the ratio of the signal at 100 m to that at 600 m from the core. The mean value according to Edge (1976) for a shower of 10^{18} eV is 145, compared with a predicted value of 370 for the present simulations.

A feature of the deep-water detector response for which no simulation results have yet given a satisfactory explanation is the insensitivity of the shape of the structure function to the primary energy of the shower. There is little change in $B(100)$ with primary energy over ~3 decades in energy (Watson, 1975; Garmston, 1976). In contrast, calculations with the scaling model indicate a change in $B(100)$ of 50% per decade around 10^{18} eV, corresponding to a steepening of the lateral distribution as energy increases. A similar steepening is a feature of several calculations based on various models (e.g., Hillas *et al.*, 1971b, and Dixon and Turner, 1974). Simulations show a strong correlation between depth of shower maximum and the deep-water detector signal near the core, but little or no correlation between depth of maximum and $\rho(600)$ (Dixon and Turver, 1974). Thus it is possible to associate the calculated increase of $B(100)$ with the approach of the average depth of shower maximum toward the observation level as shower energy increases.

Conversely, the lack of dependence of the shape of the signal on energy in observed showers would suggest that the average depth of shower maximum does not change with energy in real showers. In contrast to this expectation, Barrett *et al.* (1977) infer from measurements

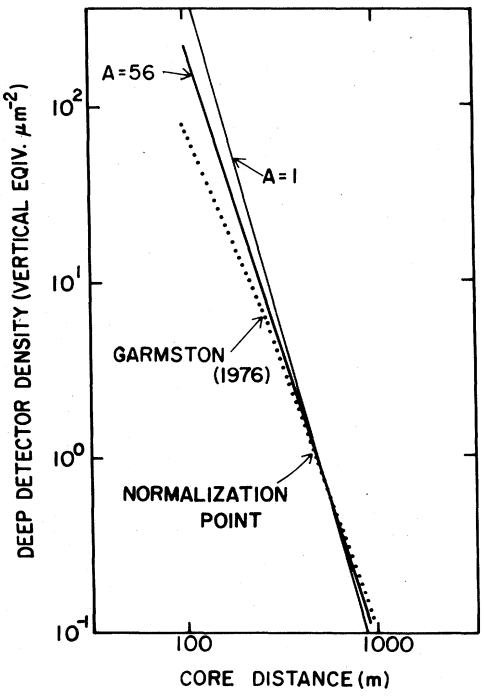

FIG. 14. The average lateral distribution for the response of the Haverah Park deep-water detectors. The solid lines show calculations, the dotted line data.

of the rise time of the signal in the deep-water detectors that the depth of shower maximum increases at the rate of 90 ± 10 gm/cm^2 per decade of primary energy. This apparent conflict between these two measures of shower development should provide a clue to the correct model of particle physics/composition. We return to this point in the discussion of implications for particle physics in Sec. V.

Barrett *et al.* (1977) have also inferred the fluctuations in depth of maximum for showers of fixed energy from observations of fluctuations from shower to shower in the rise time of the deep-water detector signal. They find $\sigma(y_{max}) \sim 70 \pm 10$ gm/cm^2 for showers of average primary energy 8×10^{17} eV. Such large fluctuations rule out a primary beam of pure heavy nuclei. Whether the fluctuations arise from an admixture of a few protons in a predominantly heavy beam or from intrinsic fluctuations in proton showers or from a combination is at present unclear. A similar result for fluctuations in N_μ for showers of fixed N_e is discussed in the next section.

F. Ratio of muon density to deep detector response

A muon-sensitive scintillation detector of large area and a deep-water detector (sensitive to muons and to the soft, electron-photon component) are collocated at the center of the Haverah Park array. The ratio of the response of the two detectors $\rho_\mu(r)/\rho_c(r)$ has been reported by Strutt (1976) for core distances, r, in the range 100-500 m. Values of this quantity for showers with $\rho(500)$ in the range 0.32–2.18 vertical equivalent muons m^{-2} are shown in Fig. 15. The response of the array (determined by the trigger and the array geometry) is such that the most probable distance of the core from the center of the array increases with the primary energy of the shower. We therefore show in Fig. 15 the dependence of $\rho_\mu(r)/\rho_c(r)$ on core distance calculated for two primary masses and energies (solid lines) and also the result of an attempt based on the known response of the Haverah Park array to take into account the likely increase of primary energy with core distance for the data (dashed line). Although a more satisfactory fit results with the heavier primary, there is still some disagreement between simulations with scaling and iron nucleus primaries, particularly near the core. However, the allowance for a systematic change in primary energy with distance clearly demonstrates the sensitivity of the shape of the $\rho_\mu(r)/\rho_c(r)$ plot to the primary energy.

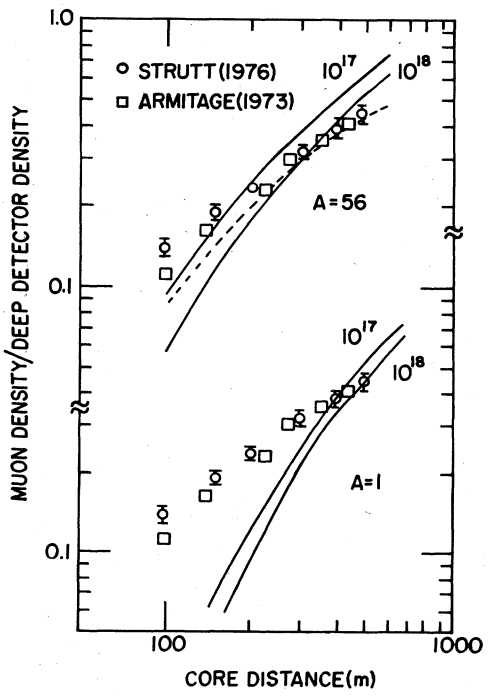

FIG. 15. The average ratio from the response of a muon sensitive detector (threshold 0.3 GeV) to that from a deep-water Čerenkov detector at various core distances. The same data are offset to show comparison with calculations for $A = 1$ and for $A = 56$. The dashed line is an attempt to take into account a triggering bias (see text).

IV. INTERPRETATION OF SHOWERS AT 10^{15} - 10^{17} eV

We now turn to smaller showers of size 10^5–10^7 particles at sea level. In the past, tests of scaling based on comparisons of calculated shower development with observational data have been made with such showers, which range in primary energy roughly from 10^{15} to 10^{17} eV. The tests have been based on average shower development (primarily the electromagnetic component), on the muon content of showers, and on certain (at present restricted) measures of fluctuations in shower properties. In this section we shall examine in some detail the extent to which various primary compositions together with scaling are consistent with EAS data in this energy range.

A. Average shower development

1. Method of constant intensity cuts

The most complete set of data that reflects average shower development in the range 10^{15}–10^{17} eV is from the Chacaltaya experiment. A revised summary of the data was presented at the Calgary Conference by La Pointe *et al.* (1968), and we adopt this as the basic data set (see Fig. 16—open circles are preliminary results reported by Bradt *et al.*, 1965). We note that Hillas (1975) has summarized measurements relevant to cascade development and that the Chacaltaya results are representative and are also the most extensive set of data.

It is important to emphasize that the development curves in Fig. 16 are not directly observed averages for groups of showers of fixed primary energies. Because any array must be at a fixed depth in the atmosphere (530 gm/cm^2 in this case) the information about longitudinal development must be obtained indirectly. This has been done by selecting showers incident from different zenith angles (and hence observed at various atmospheric depths along the shower axis). The showers are grouped in families with the same frequency. Shower development can be obtained in this way for depths ranging from the vertical depth of the array, $y_0 = 530$ gm/cm^2, to $y_0 \sec\theta_{max}$(~800–1200 gm/cm^2, depending here on shower

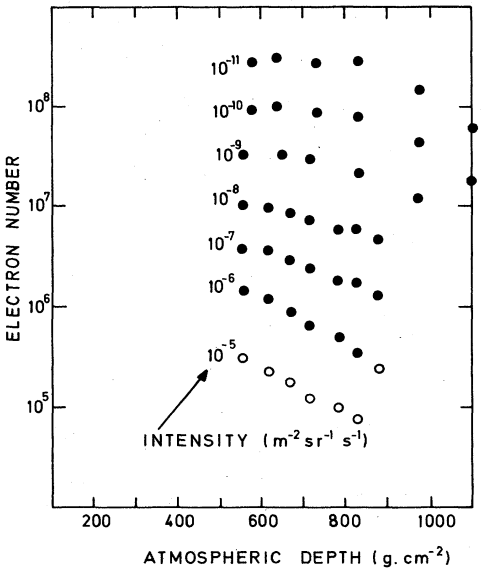

FIG. 16. The longitudinal electron cascade development. ●LaPointe *et al.* (1968); ○Bradt *et al.* (1965).

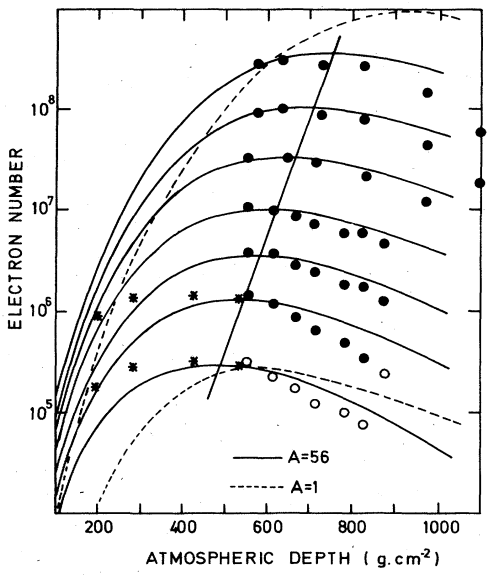

FIG. 17. The longitudinal electron cascade. The lines represent the computed values. ●LaPointe *et al.* (1968); ○Bradt *et al.* (1965), *Antonov (1974).

size). If showers at a given rate originate from primaries of similar energy, then the size versus depth curves in Fig. 16 correspond to the true average development of showers of an energy corresponding to the integral intensity $I(\mathrm{m^{-2}\ sec^{-1}\ sr^{-1}})$ in the primary spectrum.

Because of fluctuations (for example, in depth of shower initiation and in shower development) coupled with the steep primary spectrum, however, this is not the case (Dedenko, 1975). It can be shown (Gaisser and Hillas, 1977) that development curves obtained by the method of constant intensity cuts (as in Fig. 16) correspond to a good approximation to N_{rms} rather than to the average size, $\bar{N}$, of showers of fixed primary energy.

2. Comparison with calculations of longitudinal development

In view of the preceding discussion, we calculate N_{rms} for showers of fixed primary energy for comparison with the Chacaltaya curves of Fig. 16. The results are shown in Fig. 17. We have here used the model with Fe and with p primaries as described in Sec. II. The results are very similar to those first obtained by Gaisser (1974a) under essentially similar assumptions.[5] Each calculated development curve has been normalized at one depth (600 gm/cm^2). This amounts to assigning an energy to a quoted intensity (and thus calibrating the energy spectrum). The energy assignments we obtain are compared in Table I with those of Hillas (1975). Hillas' energy assignments were made primarily on the basis of considerations of ionization in a rather model-independent fashion. The close similarity between the two results suggests the absence of gross errors in the energetics of our calculation.

[5]Fe primaries combined with scaling for distributions, increasing cross section, and intranuclear cascading.

The data shown in Fig. 16 are often characterized by depth of maximum cascade development as a function of primary energy, as shown in Fig. 1. We note that the maximum is not actually seen for the lower-energy cuts in the Chacaltaya data. The only measurement of shower development that significantly extends the range of the Chacaltaya measurements is that of Antonov and Ivanenko (1973) and Antonov (1974) who have measured the size spectra of small showers at airplane altitudes (200–550 gm/cm^2), at which depth the showers have barely reached maximum. They have normalized the spectra to the two smallest constant intensity curves as reported by the Chacaltaya group at the London Conference (Bradt *et al.*, 1965). (Note that the lowest curve is based upon data later deleted from the presentation of the Chacaltaya group at Calgary.) Even though maxima are now visible for the two smallest development curves, assigning the depths of maximum for each member of the family of curves (as in Fig. 1) is still to some extent a matter of taste. For this reason we simply show the locus of the maxima of the computed showers as a solid line in Fig. 17.

Olejniczak *et al.* (1977) have, however, gone farther.

TABLE I. Energies assigned to the showers observed in the Chacaltaya experiment.

Integral flux ($m^{-2}sr^{-1}s^{-1}$)	Energy derived from energy deposition by Hillas (eV)	Energy estimate from present work (eV)
10^{-6}	$(\geq 1.9\times10^{15})$	$(\geq 1.8\times10^{15})$
10^{-7}	5.9×10^{15}	7.5×10^{15}
10^{-8}	1.6×10^{16}	1.9×10^{16}
10^{-9}	5.5×10^{16}	6.5×10^{16}
10^{-10}	1.7×10^{17}	1.9×10^{17}
10^{-11}	5.5×10^{17}	5.5×10^{17}

They have calculated a value for the effective atomic mass $A_{\rm eff}$ from a depth of maximum vs E_0 plot (including both Antonov points) by estimating what atomic mass is needed to bring their calculated depth of maximum up to the observed depth of maximum. They find a lower limit of $A = 200$. Such a calculation, however, involves exponentiating all the uncertainty and error involved in obtaining an estimate of depth of maximum from the data. This can be seen by noting that the calculated value of $y_{\rm max}$ for a nucleus of mass A is approximately given by

$$y_{\rm max} = C + B \ln(E_0/A) . \tag{4.1}$$

Then $A_{\rm eff}$ is obtained by requiring $y_{\rm max}$(calculated) = $y_{\rm max}$ (observed); i.e.,

$$A_{\rm eff} = E_0 \exp\left[\frac{C - y_{\rm max}(\text{observed})}{B}\right] , \tag{4.2}$$

where $B \sim 37$ gm/cm^2. It is therefore preferable to compare the results of a model calculation directly with the data as in Fig. 17. Clearly, the assumption of iron primaries gives significantly improved representation of this data as compared to proton primaries, although observed attenuation appears to be somewhat more rapid than the simulations. However, the lowest (10^{-5}) curve is not included in the revised data of LaPointe *et al.* (1968), and Hillas (1975) has noted previously that the next (10^{-6}) development curve may be anomalous and cannot be represented by a physical model. Some confirmation of this has recently been provided by a sea level measurement of Catz *et al.* (1975), which was not included in Hillas' summary. Moreover, a recent result from Tien Shan (Danilova *et al.*, 1977) gives attenuation from 700 to 1000 gm/cm^2 for the 10^{-6}, 10^{-7}, and 10^{-8} cuts which is significantly flatter than Chacaltaya and in good agreement with calculations for Fe and scaling.

Another way of presenting what is essentially the same data is to tabulate $N_{\rm max}/N_{\rm sea\ level}$, as has been done by Wdowczyk (1975). Directly from the data (Fig. 16), we derive the results shown in Table II. We compare our estimates of $N_{\rm max}/N_{\rm s.l.}$ with calculated values in the table. We also show for comparison the estimates made by Wdowczyk from the composite development curves of Antonov and Ivanenko (1975). As already mentioned, these were obtained by normalizing the airplane experiments (Antonov and Ivanenko, 1973; and Antonov, 1974) to the first presentation at the London Conference of the Chacaltaya data (Bradt *et al.*, 1965).

TABLE II. Calculated values of shower size at maximum to size at sea level $N_{\rm max}/N_{\rm s.l.}$ are compared to estimates based on the Chacaltaya data (LaPointe *et al.*, 1968) and estimates by Wdowczyk (1975) based on the development curves of Antonov and Ivanenko (1975).

Integral flux (m^{-2}sr^{-1}s^{-1})	Chacaltaya data	$N_{\rm max}/N_{\rm s.l.}$ Calculations Fe	p	Wdowczyk (1975)
10^{-5}	...	7.36	3.57	12
10^{-6}	13	4.82	2.16	10
10^{-7}	4.7	3.57	1.73	6.3
10^{-8}	3.5	2.70	1.45	4.3
10^{-9}	3.2	2.23	1.21	3.4
10^{-10}	2.9	1.83	1.10	
10^{-11}	2.6	1.67	1.05	

B. Muon component

1. Measurements of muon densities

It was shown in Sec. II that the muon and electron longitudinal development are fundamentally different: the muon component grows to a plateau in N_μ and then the number of muons declines rather slowly. In contrast, N_e grows to a maximum, then dies away rather rapidly (see, for example, Fig. 16). Since showers in the range 10^{15}–10^{17} eV are generally observed at sea level and are well past maximum, this means that N_μ/N_e (see Fig. 2) is in principle a sensitive measure of average longitudinal development and of fluctuations in development. However, because of large and correlated fluctuations, it is essential to be quite clear about what is actually measured.

Typical measurements of the muon flux in EAS are made with one (or at best a few) muon detectors of several tens of m^2 total area in conjunction with an array of many detectors that measures primarily the soft component. Thus, what is often measured is the muon density at a particular distance (or distances) from the shower core. For each shower the core is located by fitting the densities in the electron detectors to a semi-empirical lateral distribution, which at the same time defines N_e for the shower. Showers are then binned by N_e and a lateral distribution is built up from measurements of $\rho_\mu(r)$ at various core distances, r, in many showers in the same size bin. In this way an average muon lateral distribution characteristic of showers in a given size range is constructed.

2. Comparison with calculations of lateral distributions

The results of such an analysis for showers of size 10^5–10^6 (nominal size 2×10^5), 10^7–5×10^7 (nominal size

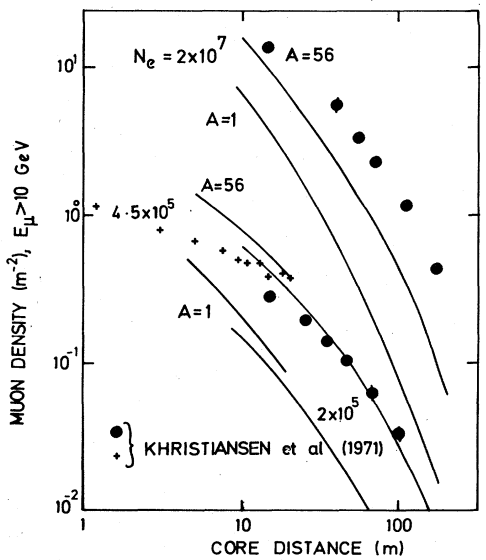

FIG. 18. The lateral distribution of muons of energy >10 GeV in showers of prescribed average size.

2×10^7), and $\geq10^5$ (nominal size 4.5×10^5), and for muons with $E_\mu>10$ GeV are shown in Fig. 18 (Khristiansen *et al.*, 1971). We have already seen in Sec. I (Fig. 2) that scaling completely fails to explain the relatively high abundance of muons if the primaries are all or mostly protons. This is again clear in Fig. 18.

3. Total muon number

It is traditional to define a total integral number of muons for each shower, $N_\mu(>E_\mu)$, by using the average distribution function described above to assign a total N_μ to each measured $\rho_\mu(r)$. In Khristiansen *et al.* (1971) this is done by scaling the measured ρ_μ up or down in energy to one of the average lateral distribution curves at $N_e=2\times10^5$ or $N_e=2\times10^7$. This is done according to $N_\mu=N_e^{0.78}$. This is the way in which the N_μ vs N_e plot shown in Sec. I (Fig. 2) was obtained.

The best fit to this data is $N_\mu(E_\mu>10\ \text{GeV})\propto N_e^{0.78}$. In contrast, scaling gives $N_\mu(E_\mu>10\ \text{GeV})\propto N_e^{0.62}$. This is illustrated by the solid lines in Fig. 2, which represent a model with scaling. As was stated earlier, a choice of proton primaries is unacceptable for these data because it gives far too few muons. It is possible that the discrepancy in slope may, to some extent, be alleviated by effects of fluctuations in the presence of a mixed primary composition, as noted below. An increasing cross section may also play a role, as would an increasing fraction of heavy nuclei (both by reducing N_e for given N_μ due to more rapid shower development at high energy). Both effects might be required since, for example, a transition from $A_{\text{eff}}<56$ at low energy to $A_{\text{eff}}\sim56$ at high energy would require a compensating increase in N_μ/N_e to keep the correct normalization in Fig. 2.

4. Fluctuations in N_μ for fixed N_e

Even though fluctuations in N_μ for fixed E_0 are expected to be relatively small, fluctuations in N_μ for fixed N_e need not be small, especially for proton primaries. This is because the steeply attenuating N_e vs depth in the region of observation is folded into the steep primary spectrum. Since N_μ is well correlated with E_0 in each shower, the fluctuations in N_e can lead to large fluctuations in N_μ for fixed N_e. Figure 19 shows the data of Vernov *et al.* (1970) for the relative dispersion σ/N_μ. Several authors (Kalmykov and Khristiansen, 1975; Olejniczak *et al.*, 1977) have pointed out that such large fluctuations rule out pure Fe composition in the range 10^{15}–10^{17} eV. Elbert *et al.* (1976) point out that there are two solutions to this problem: either a predominantly heavy composition with a small admixture of protons or a composition of nearly all protons. In the former case the fluctuations arise largely from the mixture and in the latter case largely from the large fluctuations in development characteristic of proton showers. The curves in Fig. 19 have been obtained from a scaling model by Elbert *et al.* (1976). They are able to bracket the data by varying the composition. Pure protons or pure iron primaries both give too little fluctuation. A standard mixed composition gives too much fluctuation. Predominantly iron primaries with about 10%–20% protons give agreement with the data. We have already mentioned the measurements by Barrett *et al.* (1977) of fluctuations in cascade development based on rise time of the Haverah Park deep-water detector pulses. Again, in the authors' interpretation a choice of models and masses exists to explain these data on showers of mean energy 8×10^{17} eV. One possibility is ~80% Fe and 20% protons, the other is predominantly (more than 50%) protons. The authors believe that the case of primaries being predominantly protons is preferable and that if this is so a significant departure from Feynman scaling is required to understand other EAS data.

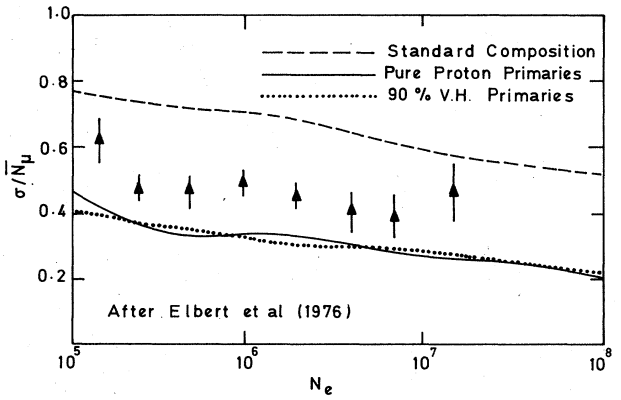

FIG. 19. The relative dispersion of muon number in showers of fixed sea level electron size.

V. IMPLICATIONS FOR PARTICLE PHYSICS ABOVE 1000 TeV

The comparisons that we have made above with EAS data fall into three groups: those that refer to measurements of properties derived from the electromagnetic component; those that reflect the muon component, in particular the low-energy muons; and those that include both. The first category is governed by the energetic π^0 component, which in turn is determined by the high-x or fragmentation region of the momentum distribution. Scaling can account for these properties provided, in some cases, that the composition is sufficiently weighted toward heavy primaries.

We have found, however, that several measurements that include effects of low-energy muons cannot be accounted for with Feynman scaling under any assumed model of primary composition. These include the lack of energy dependence of the shape of the deep-water Čerenkov signal from 10^{17}–10^{20} eV and the energy dependence of N_μ/N_e from 10^{15}–10^{17} eV (to the extent that it is not obscured by selection effects due to fluctuations in the presence of a mixed primary beam). In both cases there is in the simulations a deficiency of low-energy muons relative to electrons, which could indicate a deficiency of produced pions in the central region of the momentum distribution.[6] To test this idea, we have done

[6]The deep detector response is dominated by muons for $r>500$ m and by the electromagnetic component for $r<500$ m. Thus increasing muons relative to electrons flattens the distribution as required by Fig. 14. At the same time the relation between $\rho(500)$ and primary energy will be renormalized so that a given $\rho(500)$ corresponds to a smaller E_0.

a series of calculations based on the Landau model (Landau, 1953). This model is characterized by an energy-dependent excess of pions in the central region such that $\langle n\rangle \propto E^{1/4}$, rather than $\langle n\rangle \propto \ln E$, as for Feynman scaling. As a further test we also try a model with $\langle n\rangle \propto E^{1/3}$.

A. Landau model at EAS energies

It has been pointed out that the Landau model provides a good representation of the data in the ISR range (Andersson *et al.*, 1976). Furthermore it has been shown that the model predicts approximate scaling in the fragmentation region (Carruthers and Minh, 1973), while giving $\langle n\rangle \propto E^{1/4}$.

A simplified version of the model due to Carruthers and Minh (1973) provides a factorized form of the invariant cross section.

$$E\frac{d\sigma}{d^3p} = \frac{\sigma_{\text{inel}}\langle n\rangle B^2 e^{-Bp_T} e^{-y^2_{\text{c.m.}}/2L}}{2\pi(2\pi L)^{1/2}}\,, \tag{5.1}$$

where

$$B \approx 6(\text{GeV})^{-1}\,,$$

$$L = \tfrac{1}{2}\ln(s/4m_p^2)\,, \text{ and}$$

$$\langle n\rangle = 2E^{1/4}$$

for charged secondaries. Here $y_{\text{c.m.}} = \frac{1}{2}\ln[(E_\pi^{\text{c.m.}} + P_{\pi\parallel}^{\text{c.m.}})/(E_\pi^{\text{c.m.}} - P_{\pi\parallel}^{\text{c.m.}})]$ is the center-of-mass rapidity.

Here $F_{N\pi^c}$ can be obtained from $E(d\sigma/d^3p)$ by numerical integration of Eq. (5.1) over p_T, and it is compared for ISR energies with our standard scaling model in Fig. 20. The difference between the Landau predictions and the standard model for $x > 0.4$ is due to the fact that this simple version of the model includes some protons as well as charged pions.

We have used an even further-simplified version of the Landau model here to examine its effects on EAS calculations. The standard scaling models for $F_{N\pi}$ and $F_{\pi\pi}$ have been used for $|x| > 0.025$ but for $|x| \leq 0.025$ we set $F_{N\pi}(x) = F_{N\pi}(0)\exp(-ax^2)$ and $F_{\pi\pi}(x) = F_{\pi\pi}(0)\exp(-bx^2)$, with a and b chosen such that $F_{N\pi}(x)$ and $F_{\pi\pi}(x)$ are continuous at $x = \pm 0.025$ and $F_{N\pi}(0) = F_{\pi\pi}(0) \propto E^{1/4}$. The latter assumption gives $\langle n\rangle \propto E^{1/4}$. The distribution in energy of pions produced in π-p interactions according to this algorithm is compared in Fig. 21 to that obtained using the scaling model described in Sec. II. The distributions, which were obtained from the averages over 50 events sampled from the above distributions, illustrate how differently the two models extrapolate the same 100–1000 GeV data.

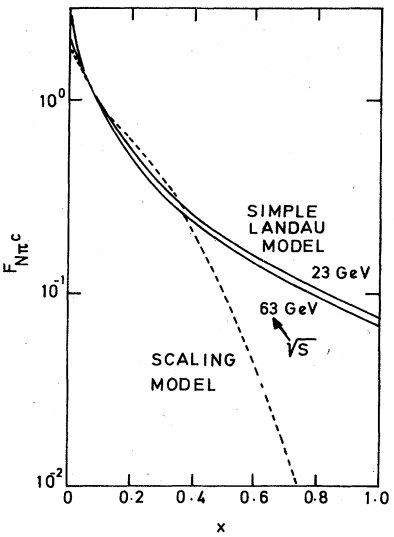

FIG. 20. The inclusive distribution for charged particle production predicted by a simple version of the Landau model at two interaction energies compared to the inclusive distribution of charged pions from the scaling model shown in Fig. 3.

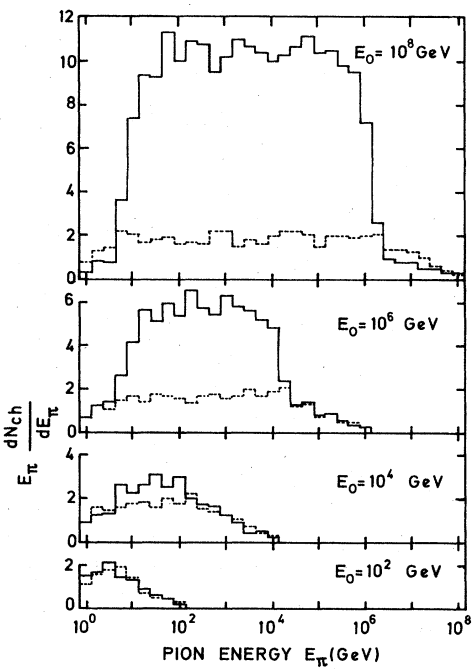

FIG. 21. The distributions in LAB energy of pions sampled from the version of the Landau model used in the present work (solid lines) compared with the distributions sampled from the scaling model at four interaction energies.

As expected, use of a model with $\langle n\rangle \propto E^{1/4}$ changes calculated results in the desired direction. In no case, however, is an acceptable fit to the data given if the primaries are protons. For Fe primaries changes to the electron cascade development are, as expected, small; typically at energies 10^{17} eV the depth of electron cascade maximum is reduced by ~50 gcm^{-2} to 640 gcm^{-2}, and this is acceptable. The muon component is enhanced by ~30% at 10^{17} eV and its energy dependence on shower size is changed to $N_\mu \propto N_e^{0.67}$, in better agreement with the data.

A version of this model with even greater enhancement of pion production in the central region, resulting in a multiplicity $\propto E^{0.33}$ has been found to give still better agreement with much of the data. Predictions illustrating this, obtained by using results from the Landau and the $E^{1/3}$ models, are given in Figs. 22–24. The data of Figs. 22 and 23 demonstrate this general improvement (see Figs. 17 and 18 for comparison). The data of Fig.

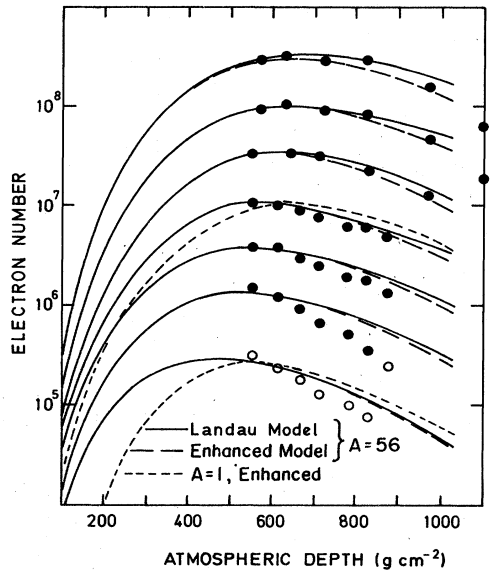

FIG. 22. The longitudinal electron cascade compared to calculations of the Landau model and a model with $\langle n\rangle \propto E^{1/3}$.

24 are perhaps of more interest in that a partial explanation is offered for the weak primary energy dependence of the shape of the Haverah Park deep detector lateral distribution. Furthermore, the altered relationship between $\rho(500)$ and primary energy is such that the measurements of Čerenkov light in showers of given $\rho(500)$ (see Fig. 9) are now more closely represented. In fact, all features of large showers that could be accounted for by Feynman scaling (Figs. 6–12) are equally well accounted for by the Landau model. However, the predicted electron lateral distribution still remains steeper than that observed.

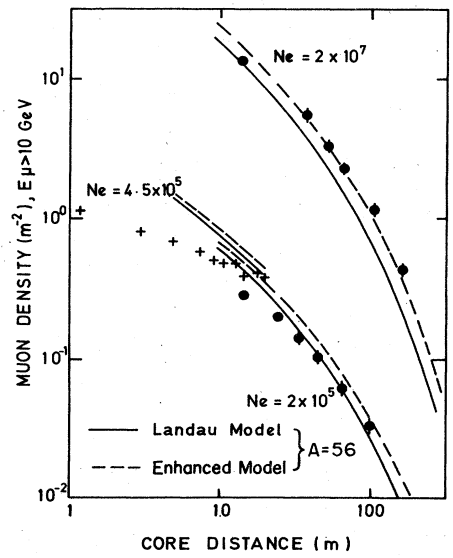

FIG. 23. The average lateral distribution of energetic muons (>10 GeV) in showers of average size 2×10^5 and 2×10^7 electrons compared to calculations of the Landau model and a model with $\langle n\rangle \propto E^{1/3}$.

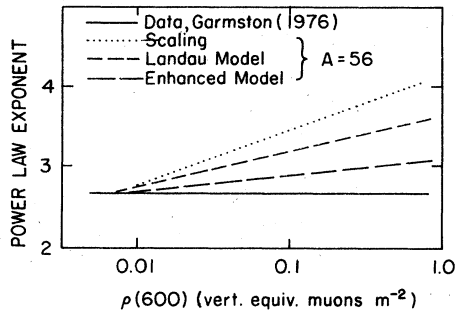

FIG. 24. The variation of the exponent of the power law representing the lateral distribution of the deep-water Čerenkov detectors with primary energy (expressed as the Haverah Park ground parameter). The data (Garmston, 1976) can be represented by an energy-independent power of ~2.67 (solid line). Calculations under various assumptions are shown.

B. Elongation rate and models

We pointed out in the introduction that many authors argue that discrepancies between scaling models and EAS data cannot be accounted for by heavy primaries alone. They argue instead that a model in which all produced pions move slowly in the center of mass is required to understand the rapid shower development and large N_μ/N_e ratio. Such a "high multiplicity model" (HMM) with $\langle n\rangle \propto E^{1/2}$ represents a drastic breakdown of scaling and is difficult to contemplate within the standard quark model of hadrons (Gaisser, 1977).

At present it is not possible to rule out a picture in which strong interactions above 1000 TeV are described by a model like HMM and in which the primaries are all, or nearly all, protons. There is, however, one measure of shower development which is independent of primary mass (provided the composition is fixed with energy over the range of interest) and which appears to favor scaling rather than HMM. This is the rate of increase of the depth of shower maximum with increasing energy.

This rate is called the elongation rate (Linsley, 1977) and is the coefficient B of $\ln E_0/A$ in Eq. (4.1). According to Linsley B is related to the rate of increase with energy of the average multiplicity by

$$B=(1-\alpha)X_0\,, \tag{5.2}$$

where $X_0 \cong 37.7$ gm/cm^2 is the electromagnetic radiation length in air and α is the exponent of E in the expression for average multiplicity in hadronic collisions

$$\langle n\rangle \propto KE^{\alpha}\,. \tag{5.3}$$

Hillas (1977) has independently found a similar, though not identical, result, which can be expressed as

$$y_{\max}=\text{const}(\bar{y}_N+\bar{y}_{\pi^\pm}+\bar{y}_{em})\,. \tag{5.4}$$

Here the constant is $\lesssim 1$ and $\bar{y}_i$ is the mean depth through which energy is transferred in the form i. Thus $\bar{y}_N=\lambda_N/K$, where λ_N is the nucleon interaction length in air and K is the inelasticity. Similarly $y_{\pi^\pm}=\frac{2}{3}\lambda_\pi/K_\pi$ and $K_\pi\sim\frac{1}{3}$ follow from assuming that one-third of produced pions are

neutral and therefore belong in the electromagnetic component. For a single π^0 it can be shown from the cascade equations for an electromagnetic cascade (Rossi and Greisen, 1941) that

$$\bar{y}_{\pi^0} = \left[0.76 + \ln\left(\frac{E_{\pi^0}}{E_{\rm crit}}\right)\right] X_0 \quad (5.5)$$

where $E_{\rm crit} \cong 77$ MeV is the critical energy characteristic of radiation theory.

To obtain $\bar{y}_{\rm em}$ for the shower as a whole, one must determine an effective π^0 energy, $E_{\pi^0}^{\rm eff}$. One retrieves the result of Linsley [Eq. (5.2)] by approximating the effective π^0 energy in Eq. (5.5) by

$$E_{\pi^0}^{\rm eff} \sim \frac{E_0}{\langle n \rangle} = \propto E_0^{1-\alpha}. \quad (5.6)$$

Note that for this approximation to be correct, the energy must be divided equally among the $\langle n \rangle$ secondary π^0's. Equation (5.2) therefore does not apply to the scaling model or to the Landau model. In the scaling model the number of π^0's effective in carrying off energy is a constant independent of E_0 so that $B_{\rm scaling} \sim X_0$. Since the Landau model has a higher multiplicity than the Feynman scaling model but still has approximate scaling in the fragmentation region, we expect $B_{\rm Landau} \lesssim B_{\rm scaling}$. (In fact, our simulations show $B_{\rm Landau}/B_{\rm scaling} \sim 0.9$.)

Experimentally, the elongation rate is usually quoted as increase in depth of maximum per decade of energy increase, i.e., $\ln 10 \times B$. For scaling-type models we thus expect a shift of $\lesssim 87$ gm/cm^2/decade whereas for the HMM, the expected shift is ~43 gm/cm^2/decade. Preliminary indications are, however, that the elongation rate is about 80–90 gm/cm^2/decade from 2×10^{17} to 5×10^{18} eV, a rate that is consistent only with models which have scaling in the fragmentation region—unless the composition changes from heavy to light as energy increases over this interval.

C. Effect of a rising cross section

Both cosmic ray (Yodh, Pal, and Trefil, 1972) and accelerator measurements (Amaldi *et al.*, 1977) suggest

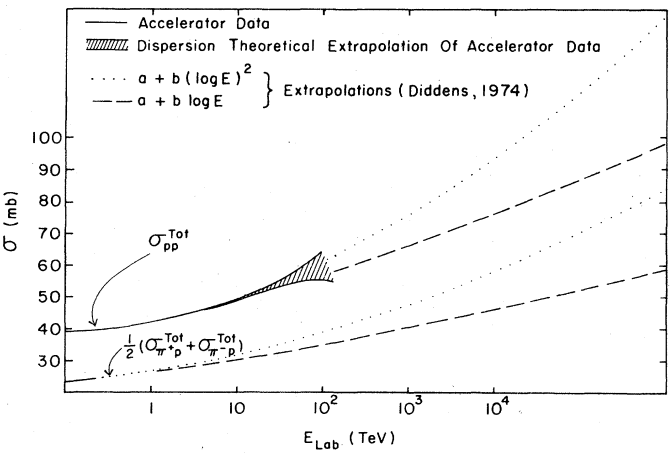

FIG. 25. Data (solid lines) and extrapolations of the cross sections for protons and for charged pions on proton targets.

TABLE III. Nucleon interaction lengths and average depth of shower maximum (in gm/cm^2) for various mean primary masses and energies and for two models of cross section.

		E_0 (eV)	10^{15}	10^{16}	10^{17}	10^{18}
	λ_N	σ = constant	80	80	80	80
		$\sigma \to (\log E)^2$	61	52	46	40
Depth of Maximum	$A=1$	σ = constant	640	750	850	930
		$\sigma \to (\log E)^2$	640	710	780	840
	$A=10$	σ = constant	...	640	750	850
		$\sigma \to (\log E)^2$	...	640	710	780
	$A=56$	σ = constant	490	550	670	775
		$\sigma \to (\log E)^2$	...	...	660	730

that the pp cross section increases over the energy range 0.1 to ~50 TeV. The value of $\sigma_{pp}^{\rm tot} \cong 55$ mb at 40 TeV corresponds to $\lambda_N \cong 73$ gm/cm^2. The behavior of σ beyond 50 TeV is an open question, but a continued increase would have the effect of shifting the shower maximum up in the atmosphere. It is therefore important to assess the extent to which this effect may be responsible for the early development of EAS.

We have used various extrapolations of the energy dependence of σ_{pp} to calculate this effect. The parametrizations of σ_{pp} and $\sigma_{\pi p}$, the resulting λ_N, and the shift in shower maximum are summarized in Fig. 25 and Table III. The standard Glauber model (Glauber and Matthiae, 1970) was used to relate $\sigma_{p\text{-}p}$ to $\sigma_{p\text{-air}}^{\rm abs}$, and $\sigma_{p\text{-air}}^{\rm inel}$ (the cross section relevant to EAS calculations) was obtained by subtracting $\sigma_{p\text{-air}}^{\rm quasielastic}$, as discussed by Gaisser *et al.* (1975). A similar procedure was used to obtain $\sigma_{\pi\text{-air}}^{\rm inel}$. The interaction lengths λ_N and λ_π were then obtained from Eq. (2.3). ($\lambda_N = 80$ gm/cm^2 corresponds to $\sigma_{pp}^{\rm tot} \cong 50$ mb.)

It is clear from Eq. (5.4) that a change $\Delta\lambda_N$ in λ_N will lead, roughly, to an equal change in depth of shower maximum for proton showers. Physically this is because the cross section affects primarily the depth of shower origin rather than the rate at which energy goes into the electromagnetic component. The results in the table confirm this.

In the table we compare results for σ = constant ($\lambda_N = 80$ gm/cm^2) with those for $\sigma \propto \ln^2 s$, the dotted extrapolation of $\sigma(E)$ shown in Fig. 25. With this increasing cross section proton primaries are still precluded by the Chacaltaya electron cascade measurements and the N_μ/N_e data. It is clear, however, from a comparison of $A=10$, rising cross section with $A=56$, σ = constant that a standard composition with $A_{\rm eff} \sim 10$ will be able to give a reasonable account of the size vs depth measurements.

VI. CONSEQUENCES FOR PRIMARY COMPOSITION

As has been illustrated repeatedly throughout the paper, it is difficult to disentangle the problem of chemical composition of the primary nuclei from questions of particle physics. We have therefore compiled a table (Table IV) that presents a matrix of implications for composition/particle physics of the various results we have referred to. Taking a conservative point of view, we ask the question "Is this primary composition compatible

TABLE IV. Can scaling be saved?

Energy range (eV)	Measurement	$A=1$	$A=10$	$A=56$	See Fig.	Comment
10^{15}–10^{18}	Long development of electron cascade	No	No	Yes?	1, 17	Also okay with increasing σ and $A=10$
10^{15}–10^{17}	Muon content	No	No	No?	2, 18	Improved by Landau model and possibly by increasing σ
2×10^{17}	Lateral distribution of low energy muons	Yes?	Yes?	Yes?	6	
10^{17}	Momentum spectra of low energy muons	No	Yes?	Yes	7	Low weight
10^{17}–10^{18}	Muon height of origin	No (by 1σ)	Yes	Yes	8	
10^{17}–10^{18}	Electron lateral distribution	No	No	Yes?	13	Calculations too steep in all cases but energy threshold uncertainties may lead to corrections that depend on radius
2×10^{17}	Air Čerenkov-lateral distribution	Yes	Yes	Yes	9	$\sigma(E)$ would flatten slightly
10^{17}–10^{20}	Response of deep water detector	No	No	No	14	Also fails for $B(100)$. Fit improved by Landau model
3×10^{17}	Shape of air Čerenkov pulse	No	?	Yes	10, 11, 12	Only top time and FWHM (Fig. 12) are sensitive to composition
10^{17}–10^{18}	Muon density/deep detector density	No	?	Yes	15	
10^{15}–10^{17}	Fluctuations in N_μ at fixed N_e	No	No	No	19	Data bracketed by standard composition and pure composition (either Fe or p). Thus a mixed composition with mostly heavy or mostly light will work

with Feynman scaling (including $\sigma=$ constant) at EAS energies?" We have attempted to answer this question for each of three primary compositions. They are $A_{\rm eff}=1$, 10, and 56. $A_{\rm eff}\sim10$ is representative of the composition around 10^{11} eV per nucleus (Juliusson, 1975), where it is directly measured. Average results for $A_{\rm eff}\sim10$ lie roughly halfway between results for $A=1$ and $A=56$. In some cases, however, fluctuations may significantly affect the analysis for a composition with a mixture of light and heavy nuclei. We return to this point below.

Early results (Gaisser and Maurer, 1972, and Wdowczyk and Wolfendale, 1972) that protons and scaling fail are clearly confirmed by a much more detailed analysis of a wider selection of data. Whether an "ordinary" composition ($A_{\rm eff}\sim10$) with scaling is viable is a more difficult question.

Several aspects of 10^{17}–10^{18} eV showers, for which pure protons and scaling fail, are better explained by scaling with $A_{\rm eff}\sim10$. The N_μ/N_e result and the average development of the electron cascade are, however, more difficult to understand in a scaling-type model with $A_{\rm eff}$ as low as 10 and not changing with primary energy. Moreover if, as is likely, $A_{\rm eff}=10$ results from a mixed composition, measurements of N_μ at fixed depth for selected N_e will see primarily proton initiated showers because of their deeper penetration superimposed on the steep primary energy spectrum. This will make an acceptable fit for the magnitude of N_μ/N_e even more difficult to achieve for $A_{\rm eff}\sim10$.

Use of the Landau model makes shower development sufficiently more rapid for proton-initiated showers so that for $A_{\rm eff}\sim10$ with a mixed composition, the development curves are in reasonable agreement with the Chacaltaya data. Similarly, an increasing cross section could decrease $y_{\rm max}$ of proton shower by as much as 40 gm/cm^2 at 10^{17} eV and thus make $A_{\rm eff}\sim10$ acceptable for this measurement. Increasing the fraction of heavies similarly improves the agreement and for the same reason.[7]

An important next step in distinguishing such possibilities is to refine calculations of the properties discussed here to take account of selection effects arising from fluctuations in the presence of a mixed composition. Indeed an important deficiency of almost all calculations thus far is lack of serious consideration of the effects of such fluctuations. This is despite the fact that a mixed composition appears to be required to account for observed fluctuations and that such a composition is likely to lead to important energy-dependent selection effects when showers are classified according to a measurement at a depth past shower maximum. For example, since proton showers penetrate farther than showers generated by heavy primaries of the same energy they will be preferentially selected because of the steep primary energy spectrum. The effect will decrease with increasing shower size as the depth of maximum comes nearer the observation level. Such a selection effect

[7]An enhancement of heavy primaries over an energy range can occur if there is a rigidity-dependent (magnetic) confinement mechanism for cosmic ray nuclei. See, for example, Peters and Westergaard (1977). Indeed, the simplest possible assumption, that all species have the same rigidity spectrum as each other and that the spectrum steepens at $\sim3\times10^6$ GV, leads to a transition from $A_{\rm eff}\sim10$ below 10^{15} eV to $A_{\rm eff}\sim25$ above 10^{17} eV.

could be the source of some part of the discrepancy between the calculated and observed slope of N_μ vs N_e in Fig. 2.

VII. CONCLUSION

No model of primary composition and particle physics has yet been shown to be entirely consistent with all reported air shower data. A great deal of the evidence is, however, consistent with scaling to 1000 TeV and above, provided in some cases that the model is modified to give a rising plateau in the central region (e.g., the Landau model) and/or an increasing cross section above 50 TeV in order to obtain a somewhat higher ratio of low-energy muons to electrons. Some experimental results (e.g., the magnitude of N_μ/N_e) also appear to require heavy primaries.

Thus scaling, at least in the fragmentation region, cannot be ruled out by existing EAS data and calculations. Conversely, scaling with proton primaries from 10^{15}–10^{18} eV is definitely ruled out by all considerations. On the other hand, it is possible that there are significant violations of scaling in the fragmentation region somewhere between 10 and 1000 TeV and that such a breakdown of limiting fragmentation is the origin of discrepancies between calculated air showers generated by protons and observed EAS. For example, Centauro-type interactions in which many hadrons but no π^0's are produced (Lattes *et al.*, 1975, and Gaisser and Yodh, 1978) would look like interactions of heavy primaries. If the cross section for such interactions were a significant fraction of the total cross section above 1000 TeV this would explain some of the features of EAS associated with their early development.

While this and other results (such as the long-flying component of Yakovlev *et al.*, 1977) suggest a significant threshold around 100 TeV, many readers may want to adopt the more conservative position that limiting fragmentation is valid and that discrepancies with experiments are to be attributed, e.g., to failure of Feynman scaling at $x=0$, increasing cross section, an increasing proportion of heavy primaries, as well as possible fluctuation effects not properly accounted for in existing calculations.

It is possible that the situation may be clarified by further calculations and comparisons to existing EAS data, particularly when attention is given to effects of fluctuations. More likely, however, a resolution of the ambiguity must await qualitatively new experiments that can give prior identification of the primary particle mass. Hitherto this has been made impossible by the low flux of primaries with $E \gtrsim 10^{15}$ eV, which has prevented their direct observation by a conventional balloon or satellite-borne detector with the capability to measure Z. A new generation of air shower experiments, designed to monitor fluctuations in longitudinal development of showers of energy $>10^{17}$–10^{18} eV, is now beginning. These include the measurements of individual showers with a wide range of particle detectors at Haverah Park and the large new EAS array at Akeno (Kamata, 1977). In addition there are the experiments based upon detection of light produced by the shower particles in the atmosphere (Bergeson *et al.*, 1977, and Orford and Turver, 1976). These latter experiments have the potential of seeing longitudinal development of individual showers and hence of measuring directly gross features of primary composition.[8] The Fly's Eye experiment of the Utah group (Bergeson *et al.*, 1977) will see individual showers of the highest energies (up to 10^{21} eV) at large distances from the detector by tracking scintillation light produced along the shower axis. The experiment of Orford and Turver reconstructs linear development of showers of somewhat lower energy (10^{17}–10^{18} eV) from pulse profiles of Čerenkov light in an array of detectors.

Finally, we point out that when general features of hadronic interactions are measured with the next generation of accelerators [ISABELLE at Brookhaven (Hahn, Month and Rau, 1977) and $p\bar{p}$ colliding beam or collider/doubler at Fermilab (Wilson, 1977)] it will be possible to infer rather directly the gross features of cosmic ray composition around 10^{15} eV.[9] It should, by comparing observed cascades with those calculated from known particle physics, be possible to determine $A_{\rm eff}$, to note whether there are two dominant mass groups and, if so, to estimate their ratios. It is unlikely that the composition could be determined in more detail than this.

After this work was completed we received a paper by Ouldridge and Hillas (1978) in which it is shown that an improved fit to the data on N_μ vs N_e can be obtained with Feynman scaling (for both slope and magnitude) for an ordinary mixed composition and a galactic steepening at 2.5×10^{15} eV per nucleon (see Footnote 7) provided the cross section continues to increase with energy as shown in the $(\log E)^2$ extrapolation of Fig. 25. Taking account of kaon and $N\bar{N}$ production leads to some increase in the slope of N_μ vs N_e as does the increasing cross section. Under the same assumptions they also find no inconsistency with the shower development curves. In this case, however, they have also used recent data from Tien Shan (Danilova *et al.*, 1977) which shows small showers developing somewhat less rapidly than the Chacaltaya data. Ouldridge and Hillas also comment on the discrepancy between measured high-energy hadrons in EAS and those calculated using scaling (Kalmykov and Khristianson, 1975). Because of inconsistencies between data from various measurements of energetic hadrons (which are in some cases larger than the discrepancy between observation and calculation) we have not dealt with this problem here. Ouldridge and Hillas also refer to the discrepancies among measurements and then compare with another new result from Tien Shan (Romankhin *et al.*, 1977) which shows good agreement with their calculations for $0.5 \lesssim E_{\rm hadron} \lesssim 10$ TeV. These results of Ouldridge and Hillas strengthen the conclusion that existing

[8] This statement assumes that heavy primaries exhibit small fluctuations and that proton showers show large fluctuations in depth of initiation (due to their relatively small cross section) and in development after initiation. Interpretation of these and other fluctuation experiments could clearly be obscured by excessively large $\sigma_{p\text{-air}}$ and a large fraction of Centauro events, which masquerade as heavy nuclei.

[9] For a review of the astrophysical context, including origin, acceleration, and propagation of cosmic rays, in which a knowledge of primary composition is important, we refer the reader to the review of Hillas (1975).

EAS data do not require a drastic failure of Feynman scaling in the fragmentation region.

ACKNOWLEDGMENTS

One of us (RJP) has been the recipient of a United Kingdom Science Research Council studentship, which is gratefully acknowledged. This work has been supported in part by the University of Durham and the U. K. Science Research Council (RJP, KET and TJLM) and by the U. S. National Science Foundation (TKG).

REFERENCES

Allan, H. R., C. J. Crannell, P. F. Shutie, and M. P. Sun, 1975, in the *Proceedings of the 14th International Cosmic Ray Conference*, Munich (Max Planck Institute, Munich), Vol. 6, p. 3071.

Amaldi, U., R. Biancastelli, C. Bosio, G. Matthiae, J. V. Allaby, W. Bartel, G. Cocconi, A. N. Diddens, R. W. Dobinson, and A. M. Wetherell, 1973, Phys. Lett. B **44**, 112.

Amaldi, U., G. Cocconi, A. N. Diddens, R. W. Dobinson, J. Dorenbosch, W. Dunker, D. Gustavson, J. Meyer, K. Potter, A. M. Wetherell, A. Baroncelli, and C. Bosio, 1977, Phys. Lett. B **66**, 390.

Amendolia, S. R., *et al.*, 1973, Phys. Lett. B **44**, 119.

Andersson, B., 1976, in the *Proceedings of the VIIth International Colloquium on Multiparticle Reactions*, Tutzing (Max Planck Institute, Munich), p. 109.

Andersson, B., G. Jarlskog, and G. Damgaard, 1976, Nucl. Phys. B **112**, 413.

Antonov, R. A., and I. P. Ivanenko, 1973, Sov. J. Nucl. Phys. **18**, 554.

Antonov, R. A., 1974, Sov. J. Nucl. Phys. **19**, 1053.

Antonov, R. A., and I. P. Ivanenko, 1975, in the *Proceedings of the 14th International Cosmic Ray Conference*, Munich (Max Planck Institute, Munich), Vol. 8, p. 2708.

Armitage, M. L., 1973, Ph. D. Thesis, University of Nottingham, England.

Atrashkevich, V. B., O. V. Vedeneev, G. V. Kulikov, V. I. Solovjeva, and G. B. Khristiansen, 1977, in the *Proceedings of the 15th International Cosmic Ray Conference*, Plovdiv (Bulgarian Academy of Science, Sophia), Vol. 8, p. 142.

Barrett, M. L., R. Walker, A. A. Watson, and P. Wild, 1977, in the *Proceedings of the 15th International Cosmic Ray Conference*, Plovdiv (Bulgarian Academy of Science, Sophia), Vol. 8, p. 172.

Baxter, A. J., 1969, J. Phys. A **2**, 50.

Benecke, J., T. T. Chou, C. N. Yang, and E. Yen, 1969, Phys. Rev. 188, 2159.

Bergeson, H. E., G. L. Cassiday, T.-W. Chiu, D. A. Cooper, J. W. Elbert, E. C. Loh, D. Steck, W. J. West, J. Linsley, and G. W. Mason, 1977, Phys. Rev. Lett. **39**, 847.

Berlad, G., A. Dar, and G. Eilam, 1976, Phys. Rev. D **13**, 161.

Boley, F. I., 1964, Rev. Mod. Phys. **36**, 792.

Bourdeau, M.-F., J. N. Capdevielle, and J. Procureur, 1977, in the *Proceedings of the 15th International Cosmic Ray Conference*, Plovdiv (Bulgarian Academy of Science, Sophia), Vol. 8, p. 332.

Bradt, H., G. Clark, M. La Pointe, V. Domingo, I. Escobar, K. Kamata, K. Murakami, K. Suga, and Y. Toyoda, 1965, in the *Proceedings of the 9th International Conference on Cosmic Rays*, London (Institute of Physics and Physical Society, London), Vol. 2, p. 715.

Butcher, J. C., and H. Messel, 1960, Nucl. Phys. **20**, 15.

Capella, A., and A. Krwczyki, 1977, Phys. Lett. B **67**, 84.

Carruthers, P., and Minh Duong-van, 1973, Phys. Rev. D **8**, 859.

Catz, Ph., J. Gawin, B. Grochalska, J. Hibner, J. P. Hochart, G. Milleret, J. Stanczyk, and J. Wdowczyk, 1975, in the *Proceedings of the 14th International Cosmic Ray Conference*, Munich (Max Planck Institute, Munich), Vol. 12, p. 4329.

Chudakov, A. G., N. M. Nesterova, V. I. Zatsepin, and E. I. Tukish, 1960, in the *Proceedings of the Moscow Cosmic Ray Conference*, Moscow, edited by G. B. Zhdanov, Vol. 2, p. 50.

Cleghorn, J. F., P. S. Freier, and C. J. Waddington, 1968, Can. J. Phys. **46**, S572.

Danilova, T. V., N. V. Kabanova, N. M. Nesterova, N. M. Nikolskaya, S. I. Nikolsky, L. M. Katsarky, I. N. Kirov, J. N. Stamenov, and V. D. Janminchev, 1977, in the *Proceedings of the 15th International Cosmic Ray Conference*, Plovdiv (Bulgarian Academy of Science, Sophia), Vol. 8, p. 129.

de Beer, J. F., B. Holyoak, J. Wdowczyk, and A. W. Wolfendale, 1966, Proc. Phys. Soc. Lond. **89**, 567.

Dedenko, L. G., 1975, in the *Proceedings of the 14th International Cosmic Ray Conference*, Munich (Max Planck Institute, Munich), Vol. 8, p. 2857.

Diddens, A. N., 1974, in the *Proceedings of the 17th International Conference on High Energy Physics, London* (Science Research Council, Rutherford Laboratory, Chilton, England), p. 1–41.

Diminstein, O. C., V. A. Kolosov, D. D. Krasilnikov, A. I. Kuzmin, V. P. Kulakovskaya, V. A. Orlov, I. Y. Sleptsov, N. N. Yefimov, and T. A. Yegorov, 1972, paper presented at the 3rd European Symposium on Air Showers and High Energy Interactions, Paris, September 1972.

Dixon, H. E., J. C. Earnshaw, J. R. Hook, J. H. Hough, C. J. Smith, W. Stephenson, and K. E. Turver, 1974, Proc. R. Soc. A **339**, 133.

Dixon, H. E., A. C. Machin, D. R. Pickersgill, G. J. Smith, and K. E. Turver, 1974, J. Phys. A **7**, 1010.

Dixon, H. E., and K. E. Turver, 1974, Proc. R. Soc. A **339**, 171.

Dixon, H. E., K. E. Turver, and C. J. Waddington, 1974, Proc. R. Soc. A **339**, 157.

Earnshaw, J. C., A. C. Machin, D. R. Pickersgill, and K. E. Turver, 1973, J. Phys. A **6**, 1244.

Edge, D. M., 1976, J. Phys. G **2**, 433.

Edge, D. M., A. C. Evans, H. J. Garmston, R. J. O. Reid, A. A. Watson, J. G. Wilson, and A. M. Wray, 1973, J. Phys. A **6**, 1612.

Edge, D. M., H. J. Garmston, R. J. O. Reid, A. A. Watson, J. G. Wilson, and A. M. Wray, 1973, in the *Proceedings of the 13th International Cosmic Ray Conference*, Denver (University of Denver), Vol. 4, p. 2513.

Efimov, N. N., D. D. Krasilnikov, G. B. Khristiansen, F. V. Shikalov, and A. I. Kuzmin, 1973, in the *Proceedings of the 13th International Cosmic Ray Conference*, Denver (University of Denver), Vol. 4, p. 2378.

Elbert, J. W., G. W. Mason, J. L. Morrison, and V. S. Narasimham, 1976, J. Phys. G **2**, 971.

Elterman, L., 1968, Air Force Cambridge Research Laboratory AFC RL-68-0153.

Feynman, R. P., 1969, Phys. Rev. Lett. **23**, 1415.

Fishbane, P. M., T. K. Gaisser, R. H. Maurer, and J. S. Trefil, 1974, Phys. Rev. D **9**, 3083.

Freier, P. S., and C. J. Waddington, 1975, Astrophys. Space Sci. **38**, 419.

Gaisser, T. K., 1974a, Nature (Lond.) **248**, 122.

Gaisser, T. K., 1974b, J. Franklin Inst. **298**, 271.

Gaisser, T. K., 1977, Rapporteur lecture, 15th International Cosmic Ray Conference, Plovdiv, to be published.

Gaisser, T. K., and A. M. Hillas, 1977, in the *Proceedings of the 15th International Cosmic Ray Conference*, Plovdiv (Bulgarian Academy of Science, Sophia), Vol. 8, p. 53.

Gaisser, T. K., and R. H. Maurer, 1972, Phys. Lett. B **42**, 444.

Gaisser, T. K., R. J. Protheroe, and K. E. Turver, 1977, in

the *Proceedings of the 15th International Cosmic Ray Conference*, Plovdiv (Bulgarian Academy of Science, Sophia), Vol. 8, p. 314.
Gaisser, T. K., and Paul Rudolf, 1976, J. Phys. G **2**, 781.
Gaisser, T. K., and G. B. Yodh, 1978, in preparation; see also Gaisser, 1977, and Yodh, 1977.
Galbraith, W., and J. V. Jelley, 1953, Nature (Lond.) **171**, 349.
Garmston, H. J., 1976, Ph. D. Thesis, University of Leeds, England. See also Edge, Garmston, *et al.*, 1973.
Glauber, R. J., and G. Matthiae, 1970, Nucl. Phys. B **21**, 135.
Grieder, P. K. F., 1977a, Rev. Nuovo Cimento **7**, 1.
Grieder, P. K. F., 1977b, in the *Proceedings of the 15th International Cosmic Ray Conference*, Plovdiv (Bulgarian Academy of Science, Sophia), Vol. 8, p. 362.
Hahn, H., M. Month, and R. R. Rau, 1977, Rev. Mod. Phys. **49**, 625.
Halliwell, C., J. E. Elias, W. Busza, D. Luckey, L. Votta, and C. Young, 1977, Phys. Rev. Lett. **39**, 1499.
Hammond, R. T., K. J. Orford, R. J. Protheroe, J. A. L. Shearer, K. E. Turver, W. D. Waddoup, and D. W. Wellby, 1977, to be published.
Hammond, R. T., K. J. Orford, J. A. L. Shearer, K. E. Turver, W. D. Waddoup, and D. W. Wellby, 1977, in the *Proceedings of the 15th International Cosmic Ray Conference*, Plovdiv (Bulgarian Academy of Science, Sophia), Vol. 8, p. 281.
Hillas, A. M., 1965, in the *Proceedings of the 9th International Conference on Cosmic Rays*, London (Institute of Physics and Physical Society, London), Vol. 2, p. 758.
Hillas, A. M., 1975, Phys. Rep. **20**, 59.
Hillas, A. M., 1977, private communication.
Hillas, A. M., D. J. Marsden, J. D. Hollows, and H. W. Hunter, 1971a, in the *Proceedings of the 12th International Conference on Cosmic Rays*, Hobart (University of Tasmania, Hobart), Vol. 3, p. 1001.
Hillas, A. M., D. J. Marsden, J. D. Hollows, and H. W. Hunter, 1971b, in the *Proceedings of the 12th International Conference on Cosmic Rays*, Hobart (University of Tasmania, Hobart), Vol. 3, p. 1007.
Juliusson, E., 1975, in the *Proceedings of the 14th International Cosmic Ray Conference*, Munich (Max Planck Institute, Munich), Vol. 8, p. 2689.
Kalmykov, N. N., and G. B. Khristiansen, 1975, in the *Proceedings of the 14th International Cosmic Ray Conference*, Munich (Max Planck Institute, Munich), Vol. 8, p. 2861.
Kalmykov, N. N., G. B. Khristiansen, Yu. A. Nechin, V. V. Prosin, N. N. Efimov, and V. M. Grigoriev, 1976, paper presented at the 5th European Symposium on Cosmic Rays, Leeds, September, 1976 (unpublished preprint).
Kalmykov, N. N., G. B. Khristiansen, Yu. A. Nechin, V. V. Prosin, V. M. Grigoriev, and N. N. Efimov, 1977, in the *Proceedings of the 15th International Cosmic Ray Conference*, Plovdiv (Bulgarian Academy of Science, Sophia), Vol. 8, p. 244.
Kamata, K., *et al.*, 1977, paper presented at the 15th International Cosmic Ray Conference, Plovdiv (to be published).
Khristiansen, G. B., O. V. Vedeneev, G. V. Kulukov, V. I. Nazarov, and V. I. Solovjeva, 1971, in the *Proceedings of the 12th International Conference on Cosmic Rays*, Hobart (University of Tasmania, Hobart), Vol. 6, p. 2097.
Landau, L. D., 1953, Izv. Akad. Nauk. SSSR **17**, 51 [translated in *Collected Papers of L. D. Landau*, 1965, edited by D. Ter Haar (Gordon and Breach, New York)].
Lattes, C. M. G., *et al.* (Brazil-Japan collaboration), 1975, in the *Proceedings of the 14th International Cosmic Ray Conference*, Munich (Max Planck Institute, Munich), Vol. 7, p. 2393.
Linsley, J., 1973, in the *Proceedings of the 13th International Cosmic Ray Conference*, Denver (University of Denver), Vol. 5, p. 3212.
Linsley, J., 1977, paper presented at the 15th International Cosmic Ray Conference, Plovdiv, to be published.
McComb, T. J. L., R. J. Protheroe, and K. E. Turver, 1977, to be published.
Olejniczak, J., J. Wdowczyk, and A. W. Wolfendale, 1977, J. Phys. G **3**, 847.
Orford, K., and K. E. Turver, 1976, Nature (Lond.) **264**, 727.
Ouldridge, M., and A. M. Hillas, 1978, J. Phys. G **4**, L 35.
Peters, B., and N. J. Westergaard, 1977, Astrophys. Space Sci. **48**, 21.
La Pointe, M., K. Kamata, J. Gaebler, L. Escobar, V. Domingo, K. Suga, K. Murakami, Y. Toyoda, and S. Shibata, 1968, Can. J. Phys. **46**, S68.
Romakhin, V. A., N. M. Nesterova, and A. G. Dubovy, 1977, in the *Proceedings of the 15th International Cosmic Ray Conference*, Plovdiv (Bulgarian Academy of Science, Sophia), Vol. 8, p. 107.
Rossi, B., and K. Greisen, 1941, Rev. Mod. Phys. **13**, 240.
Strutt, R. B., 1976, Ph.D. Thesis, University of Nottingham, England.
Tennant, R. M. 1967, Proc. Phys. Soc. Lond. **92**, 622.
Tomaszewski, A., and J. Wdowczyk, 1975, in the *Proceedings of the 14th International Cosmic Ray Conference*, Munich, (Max Planck Institute, Munich), Vol. 8, p. 2899.
Towers, L., 1971, Ph.D. Thesis, University of Leeds, England.
Turver, K. E., 1975, in the *Proceedings of the 14th International Cosmic Ray Conference*, Munich (Max Planck Institute, Munich), Vol. 8, p. 2851.
Vernov, S. N., *et al.*, 1970, Acta Phys. Hung. **29**, Supp. 3, 429.
Vernov, S. N., G. B. Khristiansen, A. T. Abrosimov, N. N. Kalmykov, G. V. Kulikov, V. I. Solovieva, Yu. A. Fomin, and B. A. Khrenov, 1977, in the *Proceedings of the 15th International Cosmic Ray Conference*, Plovdiv (Bulgarian Academy of Science, Sophia), Vol. 8, p. 320.
Watson, A. A., 1975, Izv. Acad. Nauk SSSR Ser. Fiz. **39**, p. 1215.
Wdowczyk, J., 1975, in the *Proceedings of the 14th International Cosmic Ray Conference*, Munich (Max Planck Institute, Munich), Vol. 11, p. 4002.
Wdowczyk, J., and A. W. Wolfendale, 1972, Nature (Lond.) **236**, 29.
Wdowczyk, J., and A. W. Wolfendale, 1973, J. Phys. A **6**, 1594.
Weinberg, S., 1977, Phys. Today, April, p. 42.
Whitmore, J., 1976, Phys. Rep. **27**, 187.
Wilson, Robert R., 1977, Phys. Today, October, p. 23.
Yakovlev, V. I., S. I. Nikolsky, and V. P. Pavluchenko, 1977, in the *Proceedings of the 15th International Cosmic Ray Conference*, Plovdiv (Bulgarian Academy of Science, Sophia), Vol. 7, p. 115.
Yodh, G. B., 1977, in *Prospects for Strong Interaction Physics at ISABELLE*, edited by D. P. Sidhu and T. L. Truman (BNL, New York).
Yodh, G. B., Yash Pal, and J. S. Trefil, 1972, Phys. Rev. Lett. **28**, 1005.